PCP
PLANT & CELL PHYSIOLOGY

Editing strigolactone biosynthesis genes in tomato reveals novel phenotypic effects and highlights *D27* as a breeding target for parasitic weed resistance

Alessandro Nicolia[1,*], Alessia Cuccurullo[1,2], Kento Tamada[3], Kaori Yoneyama[3,4], José Luis Rambla[5], Antonio Granell[6], Francesco Camerlengo[1], Giovanna Festa[1], Gianluca Francese[1], Felice Contaldi[1], Antonietta D'Alessandro[1], Maria Manuela Rigano[2], Luigia Principio[2], Nunzio D'Agostino[2] and Teodoro Cardi[1,7]

[1]CREA, Research Centre for Vegetable and Ornamental Crops, Via dei Cavalleggeri 51, 84098 Pontecagnano, SA, Italy, [2]Department of Agricultural Sciences, University of Naples Federico II, piazza Carlo di Borbone 1, 80055 Portici, NA, Italy, [3]Graduate School of Agriculture, Ehime University, 3-5-7 Tarumi, Matsuyama, Ehime, 790-8566, Japan, [4]Department of Biochemistry and Molecular Biology, Saitama University, Shimo-Okubo 255, Sakura-ku, Saitama-shi, 338-8570, Japan, [5]Department of Biology, Biochemistry and Natural Sciences, Jaume I University, Avda. Vicent Sos Baynat s/n, 12071 Castellón de la Plana, Spain, [6]Instituto de Biología Molecular y Celular de Plantas (CSIC-UPV), CPI Escalera 8E, Ingeniero Fausto Elio s/n, 46022 Valencia, Spain, [7]CNR-IBBR, Institute of Biosciences and Bioresources, Via Università 133, 80055 Portici, NA, Italy

*Corresponding author: E-mail, alessandro.nicolia@crea.gov.it

Received 19 July 2025; Accepted 27 March 2026

Abstract

Parasitic weed infestations represent an increasing threat to agriculture worldwide, especially in the Mediterranean region. *Phelipanche ramosa* (L.) and *Phelipanche aegyptiaca* (Pers.) (broomrapes) cause severe yield losses in field-grown tomato (*Solanum lycopersicum* L.). Strigolactones (SLs) are apocarotenoid phytohormones that not only play a critical role in plant physiology and development but also act as the primary germination signals for parasitic weed seeds. In this study, we generated CRISPR/Cas9 tomato knock-out (KO) lines targeting the *SlD27* gene and three other key genes involved in SL biosynthesis (*SlCCD7*, *SlCCD8*, and *SlMAX1*), all in the same genetic background. All the edited lines exhibited undetectable SL levels in root exudates, leading to a strong reduction in the *in vitro* germination of *Phelipanche* spp. seeds. Consistently, reduced parasitism was also observed *in vivo* when *Sld27* lines were tested. A comprehensive evaluation of morphological, reproductive, and fruit-related traits revealed gene-specific phenotypic effects, including changes in vegetative growth, fruit set, fruit development, and volatilome. Specifically, KO of two carotenoid cleavage dioxygenases and *SlMAX1* affected shoot architecture, fruit development, and the production of volatile organic compounds during fruit ripening. In contrast, the newly developed *Sld27* lines in this study displayed a mild phenotype generally comparable to nonedited control plants and likely due to the expression of *SlD27* paralogues. Overall, our results indicate that *SlD27* represents a promising breeding target for enhancing resistance to parasitic weeds in tomato while minimizing negative impacts on plant development and fruit quality.

Keywords: *D27* • fruit volatilome • genome editing • parasitic plants • *Phelipanche* spp. • tomato

Introduction

Parasitic weeds are plants that have partially (hemiparasites) or entirely (holoparasites) lost their autotrophic ability and depend on external hosts for water and nutrients (Vurro et al. 2019). Broomrapes (*Orobanche* and *Phelipanche* spp.), holoparasites of the *Orobanchaceae* family, establish parasitism by forming a vascular connection with host roots and are significant agricultural pests in the Mediterranean region (Cuccurullo et al. 2022). Among vegetable crops, tomato (*Solanum lycopersicum* L.) is particularly affected by *Phelipanche ramosa* (L.) and *Phelipanche aegyptiaca* (Pers.), leading to substantial yield losses (Vurro et al. 2019). To date, only moderate levels of resistance have been reported among cultivated tomato varieties (reviewed in Cuccurullo et al. 2022). Identifying novel tomato varieties/genotypes resistant to parasitic weeds is therefore highly desirable. The use of new genomic techniques, such as genome editing, could accelerate the development of resistant varieties in breeding programmes (Yıldırım et al. 2024).

Strigolactones (SLs) are carotenoid-derived phytohormones exuded by plant roots to recruit arbuscular mycorrhiza fungi under nutrient-deficient conditions (e.g. phosphorous and nitrogen). Furthermore, they serve as the primary signal inducing the germination of parasitic weed seeds (Mashiguchi et al. 2021). More than 25 distinct SLs have been identified to date. Different plant species and ecotypes produce specific SL profiles, consisting of unique types and

combinations of these molecules, which enable parasitic weeds to discriminate between host and nonhost species (Brun et al. 2021).

Perception of SLs by parasitic weeds is mediated by homologues of the *Arabidopsis* genes Dwarf14 (*D14*) and KARRIKIN INSENSITIVE 2 (*KAI2*, also known as HYPOSENSITIVE TO LIGHT, *HTL*). Interestingly, members of the *Orobanchaceae* family typically encode a single copy of *D14* but multiple copies of *KAI2* (Saucet and Shirasu 2016). This expansion of the *KAI2* gene is thought to represent an adaptive strategy that allows parasitic weeds to perceive diverse SL signals and thereby colonize a broad range of host species (Bouwmeester et al. 2021). This knowledge allowed the development of alternative control strategies based on synthetic germination stimulants. In a pilot study, their application in *Striga*-infested soils induced the lethal germination of the seeds in the absence of the host (Jamil et al. 2024).

Extensive research on SL biosynthesis has been conducted in model species (e.g. *Arabidopsis thaliana* L.) and selected crops (e.g. rice, tomato; reviewed in Al-Babili and Bouwmeester 2015, Mashiguchi et al. 2021, Dun et al. 2023).

In tomato, SLs are synthesized through a series of sequential reactions primarily localized in the plastid. The conversion of all-*trans*-β-carotene to carlactone is catalysed by a carotenoid isomerase (Dwarf27—SlD27) and two carotenoid cleavage dioxygenases (SlCCD7 and SlCCD8) (Vogel et al. 2010, Kohlen et al. 2012). Carlactone is further oxidated to carlactonic acid (CLA) by the cytosolic enzyme more axillary growth (SlMAX1) (Zhang et al. 2018). The subsequent oxidation steps, catalysed by various cytochrome P450 enzymes (e.g. SlCYP722C), produce canonical SLs, including orobanchol, didehydro-orobanchol, and solanacol (Wakabayashi et al. 2019, Wang et al. 2022).

Manipulation of SL biosynthesis, and the consequent reduction/alteration of SL release into the rhizosphere, has been shown to limit the germination of parasitic weed seeds in the soil, thereby disrupting the earliest phase of infection (i.e. the preattachment stage) (Fernández-Aparicio et al. 2016). This strategy has produced promising results in several major crops. In sorghum, for instance, mutation of the LOW GERMINATION STIMULANT 1 (*LGS1*) gene caused a shift in SL production from 5-deoxystrigol to orobanchol, resulting in a marked reduction in *Striga* seed germination (Gobena et al. 2017). Similarly, in maize, reduced activity of three distinct enzymes (ZmCYP706C37, ZmMAX1b, and ZmCLAMT1) redirected the biosynthetic flux from zealactone towards zealactonic acid and zealactol, two SLs that induce lower levels of *Striga* seed germination (Li et al. 2023a).

In tomato, genetic alterations affecting key SL biosynthetic genes (*SlCCD7*, *SlCCD8*, *SlMAX1*, and SlCYP722C) have been shown to reduce colonization by *Phelipanche* spp. However, with the notable exception of the *Slcyp722c* mutant, these modifications were frequently associated with pleiotropic effects, including enhanced shoot branching and reduced plant height (Vogel et al. 2010, Kohlen et al. 2012, Zhang et al. 2018, Wakabayashi et al. 2019).

SL transport has also emerged as a relevant target for limiting parasitic weed infection in tomatoes. Newly synthesized SLs are actively secreted in root exudates via ATP-binding cassette (ABC) transporters, primarily *ABCG44* and *ABCG45*. Disruption of this transport mechanism reduces SL availability in the rhizosphere and provides an additional layer of resistance against parasitic weeds. Nevertheless, as observed for biosynthetic mutants, impairment of SL transport is also accompanied by pleiotropic developmental effects (Bari et al. 2021b, Ban et al. 2025).

Other root-exuded molecules, such as isothiocyanates, can also stimulate parasitic seed germination and thus contribute to host root parasitism (Miura et al. 2022). In peas, reduced or absent SL exudation was not sufficient to confer complete field resistance (Arcieri et al. 2025). These findings indicate that additional stages of the parasitic weed infection process (e.g. haustorium development, postattachment) are also important in determining host resistance. Accordingly, plant species exhibiting low release of haustorium inducing factors (i.e. flavonoids, phenolic acids, and cytokinins) or those capable of blocking the nutrient flux at parasitism sites through different molecular mechanisms (Yoder and Scholes 2010) have been identified, but, so far, these findings have led to the development of few resistant varieties (reviewed in Chachalis et al. 2025).

Previous studies on the genes involved in SL biosynthesis and transport in tomato were conducted in various genetic backgrounds (reviewed in Cuccurullo et al. 2022), complicating direct comparisons of the observed phenotypes. Moreover, specific functional studies on the carotenoid isomerase D27 in tomato and other crops, as well as its relevance in conferring resistance to parasitic weeds, are still lacking.

In this study, we generated CRISPR/Cas9 tomato knockout (KO) lines for the *SlD27* gene and three other key SL biosynthetic genes (*SlCCD7*, *SlCCD8*, and *SlMAX1*) within the same genetic background. We evaluated the SL content in root exudates and assessed the germination rates of *P. ramosa* and *P. aegyptiaca* in an *in vitro* assay. An *in vivo* infection assay with *P. ramosa* was also conducted. Furthermore, to compare the effects of inactivating the different genes and assess the breeding and agronomic value of the edited lines, we performed a comprehensive characterization of morphological, reproductive, and fruit-related traits, including the characterization of the volatilome and evidencing, in comparison with *Slccd7*, *Slccd8*, and *Slmax1* mutant lines, a reduced phenotypic effect of the *Sld27* KO. Finally, the results of expression analysis of *D27* and two paralogues suggest a possible role of *D27-LIKE1* and *D27-LIKE2* genes in such a phenotype.

Results

Knockout mutants of strigolactone biosynthetic genes were efficiently generated using CRISPR/Cas9

The single-guide RNAs (sgRNAs) designed to specifically target genes involved in SL biosynthesis showed an efficiency of mutagenesis ranging from 35% to 89% in hairy root (HR) assays

mediated by *Agrobacterium rhizogenes* (Supplementary Table S1). This screening allowed us to rapidly test the sgRNAs' efficiency before approaching the lengthy regeneration protocol based on *Agrobacterium tumefaciens*. Independent transformations of tomato cotyledons using *A. tumefaciens* and the same four vectors employed in the HR assays resulted in the generation of 10 KO plant lines: two lines each for *Sld27* and *Slmax1*, and three lines each for *Slccd7* and *Slccd8* (Fig. 1). Sanger sequencing of target genes from selected T_2-generation plants (T-DNA-free) confirmed that all the edited lines were biallelic and homozygous for their respective mutations. Additionally, the presence of potential off-target effects was ruled out (Supplementary Table S2).

In the newly generated *Sld27*, *Slccd7*, *Slccd8*, and *Slmax1* lines, editing resulted in frameshift mutations, leading to KO genotypes (Fig. 1). In the *Sld27* KO lines, the limited size of the exons hampered sgRNA design, necessitating targeting of the 5′ untranslated region. A single insertion was introduced before the start codon, accompanied by either a deletion (*Sld27*-KO1) or an insertion (*Sld27*-KO2) of a single base in the second exon. The three *Slccd7* KO lines exhibited deletions in the first exon: 1 bp in *Slccd7*-KO1 and *Slccd7*-KO2, and 2 bp in *Slccd7*-KO3, whereas the three *Slccd8* KO lines displayed a broader range of deletions in the second exon: 2 bp in *Slccd8*-KO2, 4 bp in *Slccd8*-KO1, and 5 bp in *Slccd8*-KO3. Finally, the two *Slmax1*-KO lines exhibited deletions in exon 3: 1 bp in *Slmax1*-KO2 and 4 bp in *Slmax1*-KO1.

Strigolactones are undetectable in root exudates of edited tomato lines

Tomato plants produce and exude at least five SLs, including orobanchol, solanacol, 6,7-didehydroorobanchol, phelipanchol, and epihelipanchol (Zhang et al. 2018, Wakabayashi et al. 2022). Authentic standards of orobanchol and solanacol were available, allowing for their confirmation. Both SLs were readily detectable in the root exudates of control nonedited plants but were not detected in the edited tomato lines. This provided a functional confirmation that the four genes involved in the SL biosynthetic pathway were successfully knocked out by CRISPR/Cas9 (Fig. 2a and b). Authentic standards for 6,7-didehydroorobanchol, phelipanchol, and epihelipanchol were not available. Consequently, MRM channels for these SLs were set based on previously reported data (Zhang et al. 2018, Wakabayashi et al. 2022). A distinct single peak was observed exclusively in the root exudates of nonedited control plants and not in the edited lines (Fig. 2c). However, it remained unclear whether this peak corresponded to 6,7-didehydroorobanchol, phelipanchol, or epihelipanchol. Carlactone was additionally assessed in root exudates and was not detected in any of the edited tomato lines (data not shown).

Root exudates from the edited tomato lines reduced germination of root parasitic weeds

We evaluated the effects of root exudates from nonedited control plants and CRISPR/Cas9-edited lines on the germination of *P. ramosa* and *P. aegyptiaca* (Fig. 3a and b), for which tomato is a regular host, and *Orobanche minor*, usually not found in tomato fields but characterized by a high sensitivity to SL-induced germination (Takei et al. 2023) (Fig. 3c). The *Slccd7* and *Slccd8* lines were the most effective, showing a lack of stimulation of the parasite germination by >90% (Fig. 3a and b). A marked reduction in the germination of *P. ramosa* seeds was observed following treatment with *Sld27* root exudates (Fig. 3a). However, this response was less consistent in *P. aegyptiaca* seeds treated with root exudates form *Sld27*, where germination was reduced to ∼20% (Fig. 3b). Additionally, root exudates from *Slmax1* lines still appeared to stimulate higher germination percentages (Fig. 3; Supplementary Fig. S1).

An *in vivo* infection assay with *P. ramosa* was performed on *Sld27* and *Slccd7* mutants. Compared with nonedited wild-type (Wt) control plants, the *Sld27* genotype exhibited a significant reduction (∼48%) in the number of emerged shoots. An even greater reduction, ∼80%, was observed in the *Slccd7* mutants (Fig. 4a; Supplementary Table S3). In all the mutants examined, the *P. ramosa* shoots that emerged during the *in vivo* assay developed normally and produced flowers and seeds (Fig. 4b).

The *Sld27* edited tomato lines exhibit morphological, reproductive, and fruit-related traits similar to those of the wild type

The *Sld27*, *Slccd7*, *Slccd8*, and *Slmax1* CRISPR/Cas9 KO lines generated in this study were compared with the control nonedited plants by evaluating a total of 13 phenotypic traits.

Considering the morphological traits, height reduction was significant in *Slccd7*, *Slccd8*, and *Slmax1* at all sampling points, due to a reduction in internode length particularly evident at 33 days after transplanting (DAT). The increase in lateral branching was more pronounced in the *Slccd8* and *Slmax1* lines, which exhibited a doubling in the number of branches. The *Slccd7* and *Slccd8* lines showed a remarkable increase in adventitious root production compared to the control (up to 35-fold in *Slccd8*). Interestingly, the *Slmax1* lines displayed a smaller and less consistent increase in HRs (Fig. 5; Supplementary Table S4; Supplementary Fig. S2).

The analysis of reproductive traits evidenced that the *Slccd8* and *Slmax1* lines showed a significant reduction in flower numbers on the third inflorescence; notably, the *Slccd7* lines were comparable to the nonedited control plants. The *Slmax1* lines exhibited a remarkable reduction in fruit set (≤73%) a trait also found in *ccd7*-KO3, whereas the *Slccd8* lines were comparable to the control (Fig. 6; Supplementary Table S4).

Interestingly, the examination of fruit-related traits highlighted an extended period from anthesis to the onset of ripening (≤7 days) in the *Slmax1* lines. Aside from the marginal significance observed in *ccd7*-KO3, the other *Slccd7* lines, as well as the *Slccd8* lines, did not show significant changes.

The *Slmax1* lines also exhibited the most pronounced reduction in fruit weight (≤17.58 g). Similarly, two out of three *Slccd7* lines experienced a significant decrease (≤11.34 g), whereas among *Slccd8* lines, only *ccd8*-KO1 showed a significant

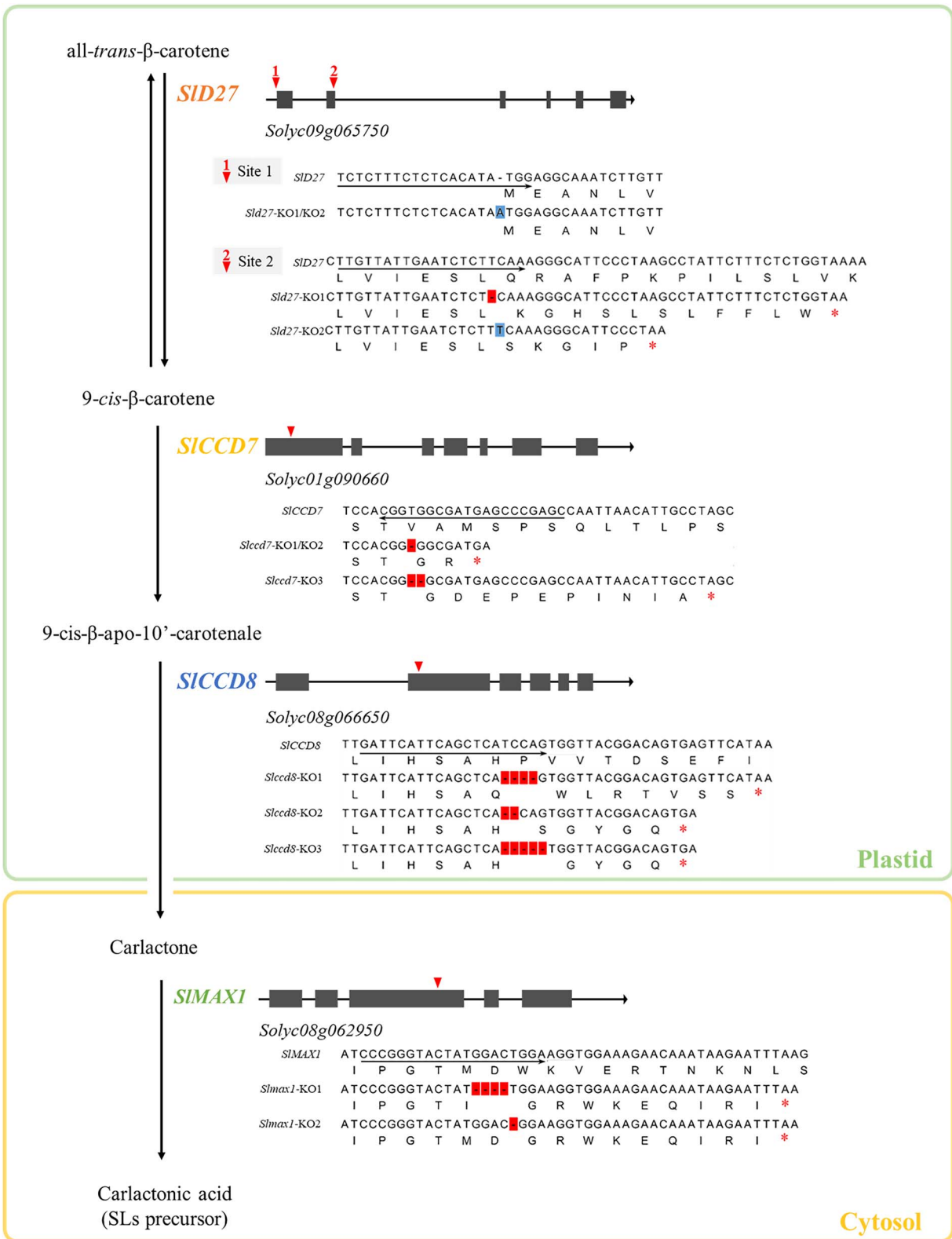

Figure 1. Schematic representation of induced mutations targeting core SL biosynthesis genes in CRISPR/Cas9-edited tomato lines. The figure provides an overview of the compartmentalized SL biosynthesis pathway in tomato, depicting the enzymatic steps from all-*trans*-β-carotene to CLA. The genomic structure of each SL biosynthesis gene is illustrated, with genes represented as arrows oriented from the 5′(left) to the 3′(right) end (not drawn to scale). Exons are shown as boxes, and the CRISPR/Cas9 target sites are marked with inverted triangles. Local alignment between the cDNA sequences of wild-type and CRISPR/Cas9 KO lines are displayed for each gene. The 20-nucleotide sgRNA sequence is underlined by a arrow below the wild-type sequence, indicating its orientation. Mutations resulting from CRISPR/Cas9 activity are highlighted in red (deletions) and blue (insertions) within the KO line sequences. Out-of-frame mutations are shown in the corresponding translated amino acid sequences below each cDNA sequence, with the premature stop codon indicated by an asterisk.

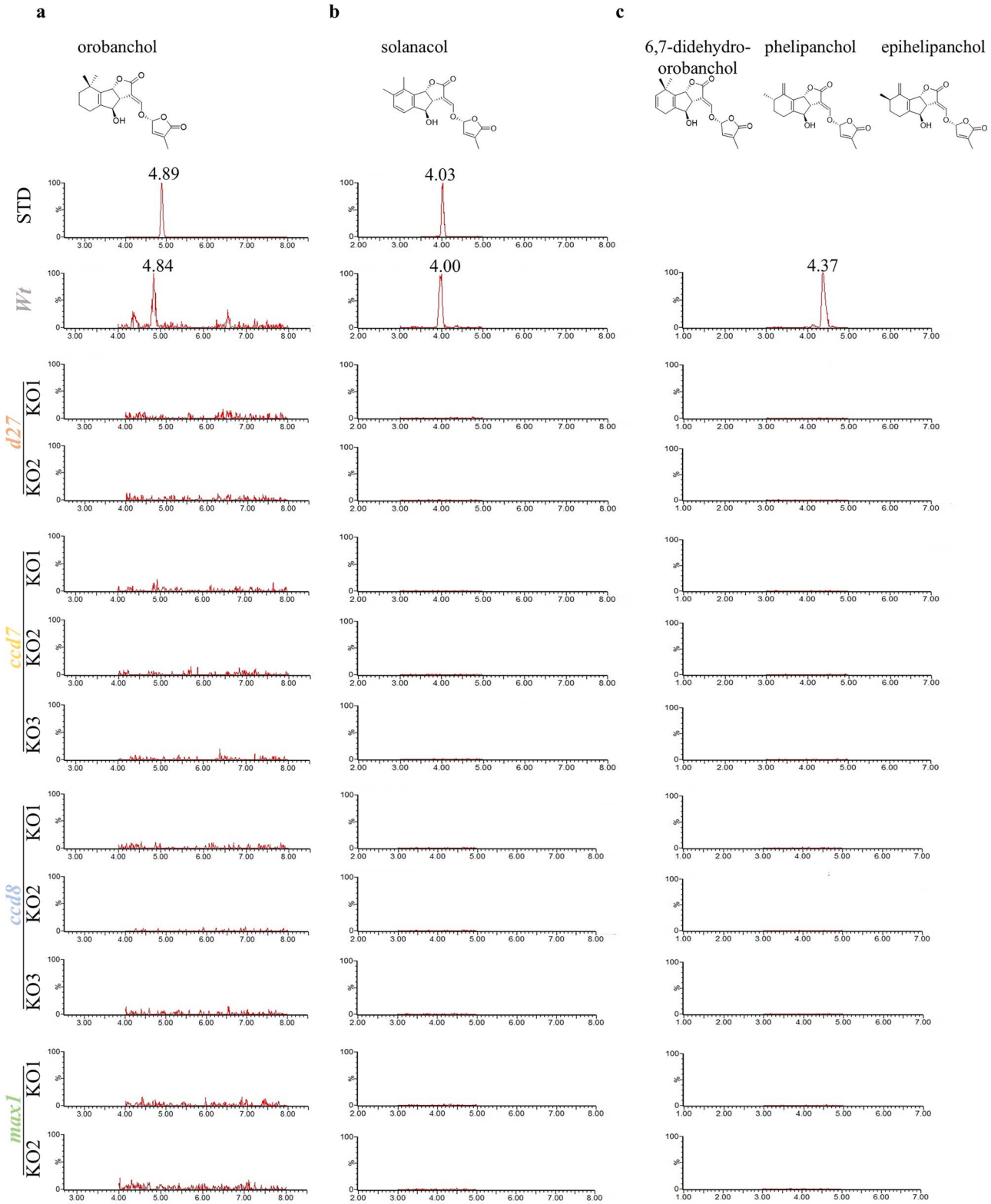

Figure 2. Detection of SLs in root exudates of nonedited control plants (wild-type, Wt) and CRISPR/Cas9 KO lines targeting core SL biosynthesis genes (*SlD27*, *SlCCD7*, *SlCCD8*, and *SlMAX1*). Quantification was performed using UPLC-MS/MS. (a) MRM chromatograms for orobanchol (*m*/*z* 347.1 → 97.0). (b) MRM chromatograms for solanacol (*m*/*z* 343.1 → 96.9). (c) MRM chromatograms for 6,7-didehydro-orobanchol, phelipanchol, and epiphelipanchol (*m*/*z* 345.1 → 97.0). *X*-axis: retention time (min); *Y*-axis: reactive intensity (%). STD: standard.

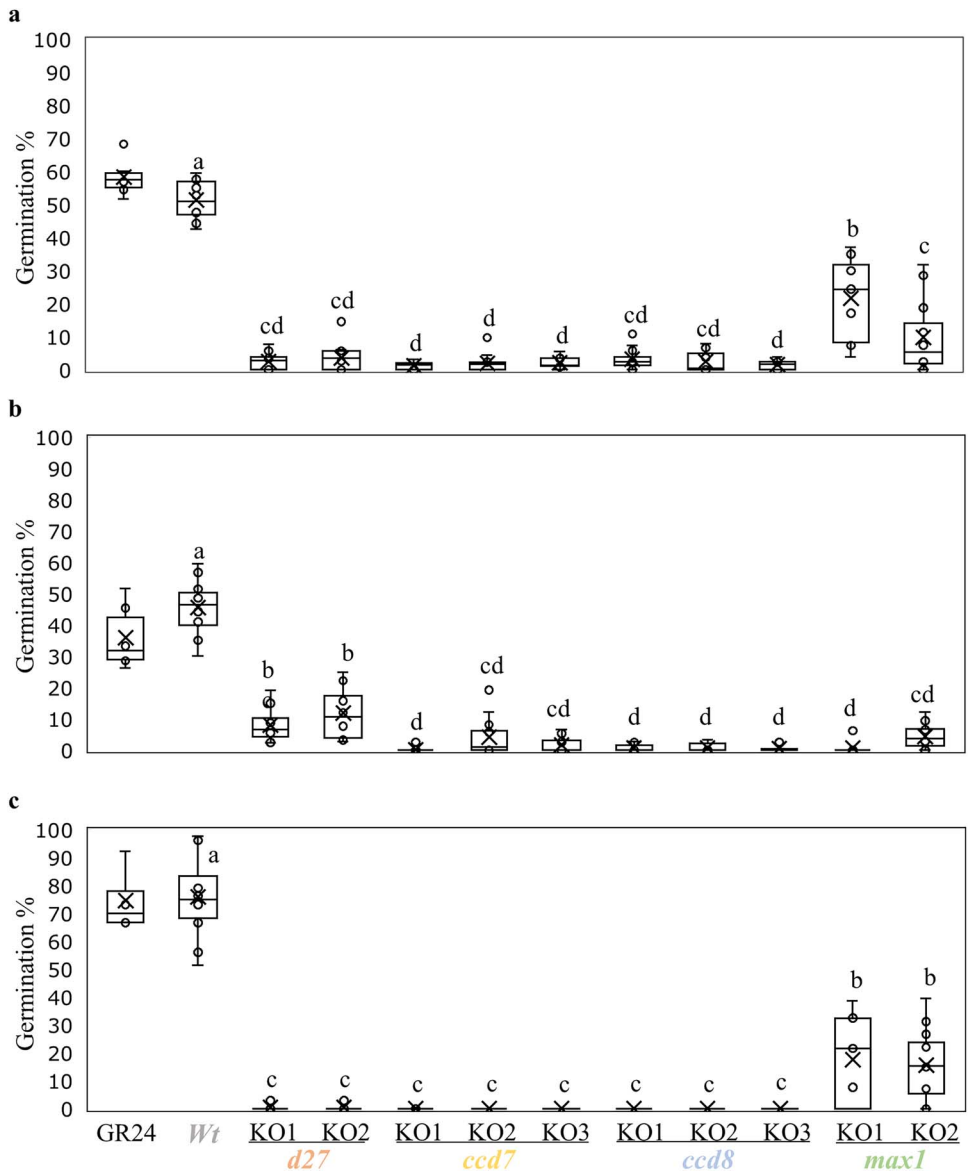

Figure 3. Germination-stimulating activity of tomato root exudates on *Phelipanche* spp. and *Orobanche minor* seeds. Root exudates were sampled from nonedited control plants (wild-type, Wt) and CRISPR/Cas9 KO lines targeting SL biosynthesis genes (for each line, $n = 3–4$). These samples were used in germination assay with seeds of *P. ramosa* (L.) (a), *P. aegyptiaca* (Pers.) (b), and *O. minor* (c). Statistically significant differences among lines are indicated by different letters ($P < 0.05$), as determined by Tukey's HSD test. GR24 (10^{-6} M) was included as the positive control in the assays.

reduction. Alterations in fruit width mirrored the changes in fruit weight, with the most severe reduction in *Slmax1* (≤0.72 cm). Fruit length was also significantly reduced, with *Slmax1* lines showing the most pronounced reduction (≤0.61 cm) (Fig. 7; Supplementary Table S4).

The *Sld27* lines generally did not show significant differences in the morphological, reproductive, and fruit-related traits compared to nonedited plants, exhibiting a mild phenotype similar to the control (Figs. 5, 6, and 7; Supplementary Table S4).

These results were largely confirmed when the 13 morphophysiological traits were subjected to linear discriminant analysis (LDA) to verify the best separation of the lines according to the linear trait combinations and rank traits for their importance in group separation. The LDA model produced two canonical variables (i.e. discriminant functions), LD1 and LD2, which explained 79.08% and 15.17% of the variance, respectively (Supplementary Table S5). Interestingly, the *Sld27* lines clustered very close to the nonedited control group (Fig. 8a) and were clearly distinguishable from the other lines (*Slccd7*, *Slccd8*, and *Slmax1*), indicating a high degree of similarity between these mutants and the control in terms of the traits evaluated. LD1 was positively correlated ($r \geq 0.60$) with plant height, average internode length, number of flowers on the third inflorescence, and fruit weight. Conversely, LD1 was

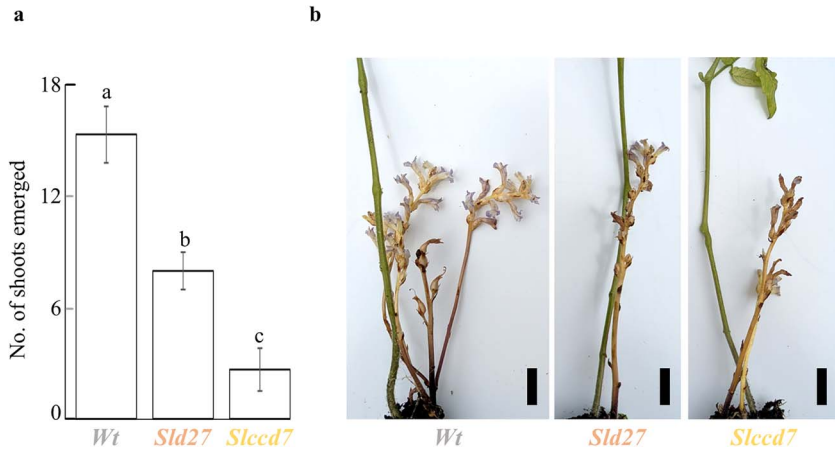

Figure 4. *In vivo* infection assay with *P. ramosa* seeds. (a) Cumulative number of *P. ramosa* shoots that emerged per plot (10 plants per plot) for nonedited wild-type (Wt) control plants and CRISPR/Cas9 KO lines *Sld27* (*d27*-KO1) and *Slccd7* (*ccd7*-KO3). Each line was tested in three independent biological replicates ($n = 3$). Different letters indicate statistically significant differences among lines ($P < 0.01$; Tukey's HSD test). Error bars represent means ± SD (see Supplementary Table S3 for details). (b) Phenotype of the *P. ramosa* shoots that emerged from a single infected plant randomly picked from the Wt, *Sld27*, and *Slccd7* plots. Scale bar = 2 cm.

negatively correlated ($r \leq -0.60$) with the number of lateral branches, number of adventitious roots, and number of days between anthesis and the breaker stage. LD2 was positively correlated with the fruit set percentage and fruit width (Fig. 8b; Supplementary Table S5).

Profiling of fruit metabolites showed differences among edited tomato lines

The *Sld27*, *Slccd7*, *Slccd8*, and *Slmax1* lines were compared with the control nonedited plants by evaluating sugar content, selected polar and nonpolar metabolites, and volatile organic compounds (VOCs) in fruits.

The analysis of variance (ANOVA) and *post hoc* analysis failed to clearly identify any specific line with differences in the average content of fructose and glucose between SL mutant lines and the control (Supplementary Table S6).

Regarding polar metabolites, quantification of chlorogenic acid (CA) showed no detectable level in *ccd7*-KO3, whereas all other lines resembled the control (Supplementary Table S7).

The analysis of the flavonoid rutin (Rut) did not reveal statistically significant differences in *post hoc* analysis between the edited lines and controls. Conversely, the flavonoid naringenin chalcone (NaCh) appeared to be generally increased but statistically significant only in *max1*-KO1 (Supplementary Table S7).

On examining nonpolar metabolites, the major carotenoids and tocopherols exhibited negligible changes, with the sole exception of the δ-tocopherol, which was reduced in *ccd8*-KO2, and the all-*trans* lycopene, which appeared slightly reduced in *max1*-KO2 (Supplementary Table S8).

The ripe fruits unequivocally revealed 64 different VOCs. Specific VOC and metabolic pathways resulted highly affected in tomato fruits by alterations in SL biosynthesis (Supplementary Table S9). Indeed, considering the benzenoid/phenylpropanoid pathway (B), eugenol, guaiacol, and methyl salicylate (MeSA) were significantly increased (≤2.02-, 2.8-, and 8-fold, respectively) in the *Slmax1* lines (Fig. 9; Supplementary Table S9). Among the branched-chain amino acid (BCAA)-related compounds, 3-methyl butanoic acid was highly reduced in *Slccd7*, *Slccd8*, and *Slmax1* (≤0.29-fold). Similarly, 1-nitro-3-methylbutane was significantly reduced in both *Slmax1* lines (≤0.12-fold) (Fig. 9; Supplementary Table S9). Within the phenylalanine derivative (Phe) group, 2-phenylethanol was reduced in the *Slccd8* and *Slmax1* lines (≤0.29- and ≤0.16-fold, respectively). These declines were more pronounced for 1-nitro-2-phenylethane, which was also affected in the *Slccd7* lines (Fig. 9; Supplementary Table S9). In contrast, the pathways of fatty acid derivatives (L), apocarotenoids (ApoC), and terpenoids (T) seemed to be not affected by mutations in SL genes (Supplementary Table S9).

LDA was performed to summarize the behaviour of the lines and confirm their separation based on VOC content, while simultaneously ranking the various compounds by their significance in group differentiation. Interestingly, the LDA identified four clusters: (i) nonedited control plants; (ii) *Sld27* lines; (iii) *Slccd7* and *Slccd8* lines; (iv) *Slmax1* lines (Supplementary Fig. S3). The canonical variable LD1 accounted for 57.19% of the variability and was positively correlated ($r \geq 0.60$) with two BCAA-related compounds (3-methylbutanoic acid and 1-nitro-3-methylbutane), one L compound (*E*-2-pentenal), and two Phe compounds (2-phenylethanol and 1-nitro-2-phenylethane). Conversely, LD1 exhibited negative correlation ($r \leq -0.60$) with two T compounds (*p*-cymene and 2-caren-10-al) (Supplementary Table S10). The second canonical variable, LD2, explained 25.69% of the variability and was negatively correlated ($r \leq -0.60$) with two B compounds (guaiacol and MeSA) and positively correlated ($r \geq 0.60$) with one BCAA-related compound (3-methylbutanenitrile) (Supplementary Fig. S3; Supplementary Table S10).

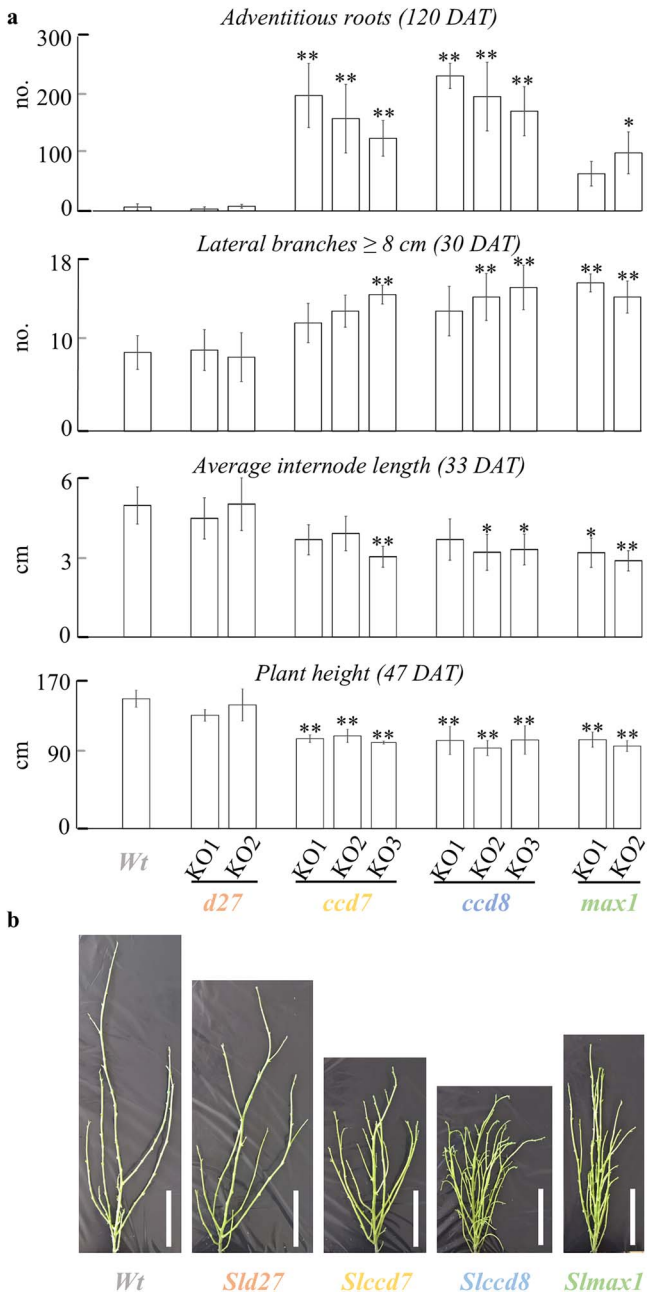

Figure 5. Variation in morphological traits of CRISPR/Cas9 KO lines targeting SL biosynthesis genes. (a) Bar charts display the mean value ± SD of the number of adventitious roots, number of lateral branches ≥ 8 cm, average internode length and plant height, in the KO lines for the four genes ($n = 4$ for each KO line). Statistical significance was determined using Tukey's HSD for comparisons with the nonedited control plants (wild-type, Wt). Significant differences are indicated with asterisks: $P \leq 0.05$ (∗); $P \leq 0.01$ (∗∗). Quantitative data for each trait were collected at specific DAT (days after transplant), which are indicated. (b) Representative images, acquired at the end of the growing cycle and from a single biological replicate, of the stem in KO lines compared to the Wt. Images are shown to scale for accurate visual comparison, with white bars representing 20 cm.

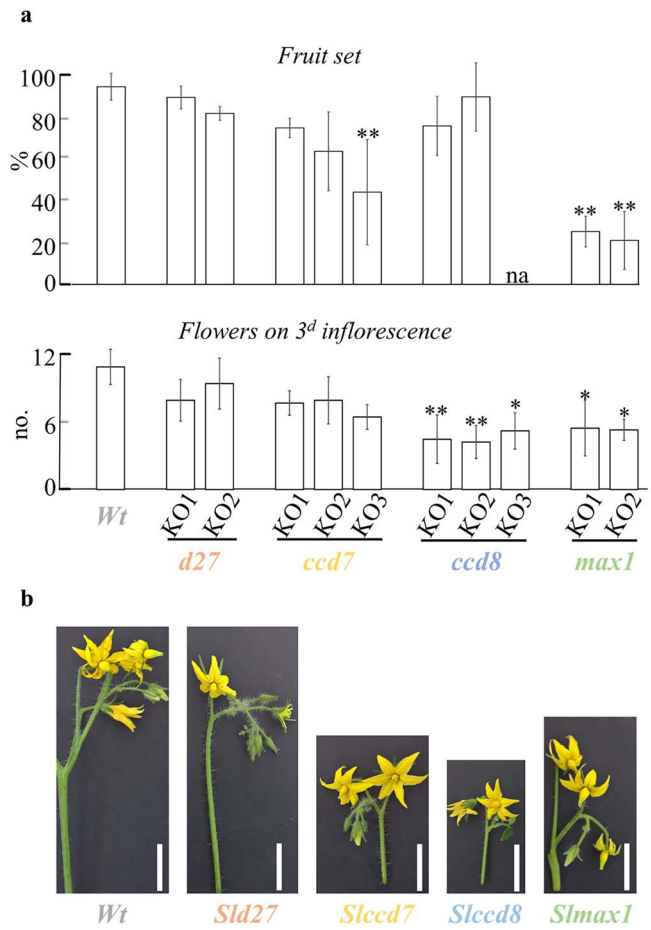

Figure 6. Variation in reproductive traits of CRISPR/Cas9 KO lines targeting SL biosynthesis genes. (a) Bar charts display the mean value ± SD of fruit set and flowers on the third inflorescence, in the KO lines for the four genes ($n = 4$ for each KO line). Statistical significance was determined using Tukey's HSD for comparisons with the nonedited control plants (wild-type, Wt). Significant differences are indicated with asterisks: $P \leq 0.05$ (∗); $P \leq 0.01$ (∗∗). na: not available. (b) Representative images of the inflorescence in KO lines compared to the Wt. Images are shown to scale for accurate visual comparison, with white bars representing 2 cm.

D27-LIKE genes were differentially expressed in leaves and roots of the *Sld27* mutant

Based on the coding and protein sequences of *SlD27-LIKE1* and *SlD27-LIKE2* retrieved from Cuccurullo et al. (2024), the presence of a 34-aa-long plastid transit peptide in SlD27-LIKE1 was predicted with high probability. Probability was lower for SlD27-LIKE2 (Supplementary Fig. S4).

To investigate potential functional redundancy among the *SlD27* and *SlD27-LIKE* genes, we determined their expression profiles in roots and leaves under low (P−) and normal (P+) inorganic phosphate conditions. First, the transcriptional response to phosphate starvation (P−) was evaluated. In the *Sld27* mutant, relative expression (RE) of *SlD27* and *SlCCD8*

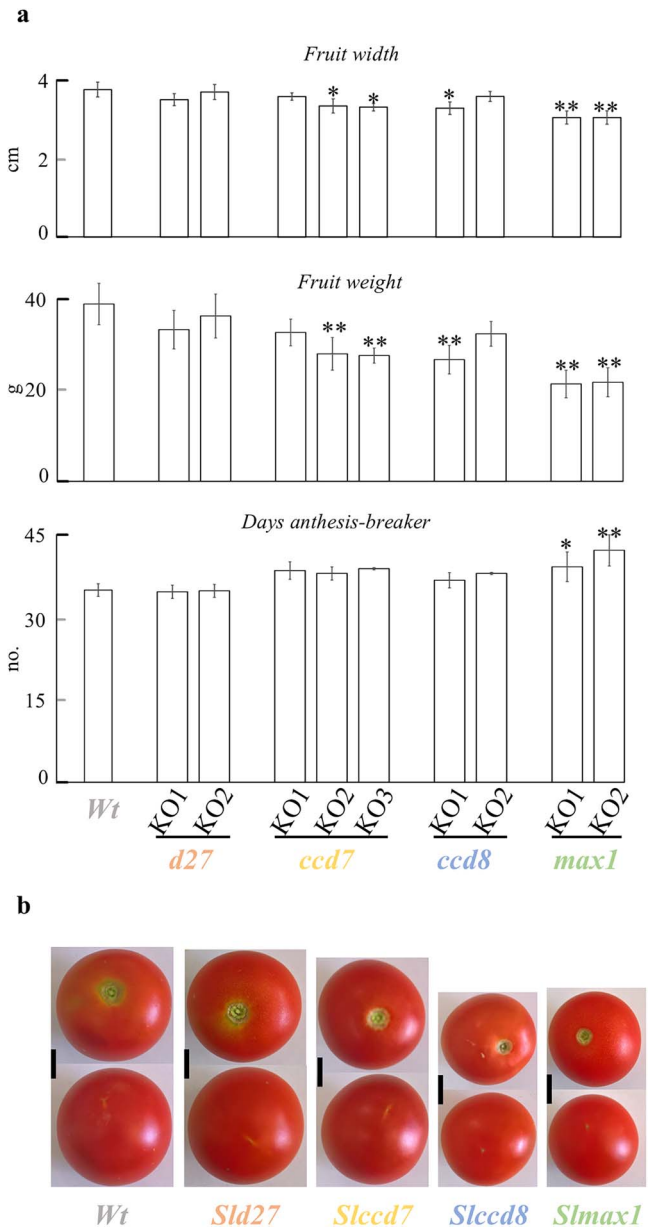

Figure 7. Variation in fruit-related traits of CRISPR/Cas9 KO lines targeting SL biosynthesis genes. (a) Bar charts display the mean value ± SD of fruit width, fruit weight, and days from anthesis to the onset of ripening (breaker) in the KO lines for the four genes ($n = 4$ for each KO line). Statistical significance was determined using Tukey's HSD for comparisons with the nonedited control plants (wild-type, Wt). Significant differences are indicated with asterisks: $P \leq 0.05$ (*); $P \leq 0.01$ (**). (b) Representative images of the fruit in KO lines compared to the Wt. Images are shown to scale for accurate visual comparison, with the vertical black bar representing 1 cm.

increased by ∼12-fold and 27-fold, respectively, in roots. The presence of *SlD27* and *SlCCD8* mRNA was detected also in leaves in P− condition; however, RE values could not be determined because transcripts were undetectable under P+ condition (Fig. 10a; Supplementary Table S11a). In contrast, *SlD27-LIKE1* responded to P− with approximately a two-fold reduction in root expression and a moderate increase in leaf expression (∼1.4-fold). Conversely, *SlD27-LIKE2* exhibited an ∼1.9-fold increase in expression in both roots and leaves (Fig. 10a; Supplementary Table S11a). Nonedited Wt plants displayed expression patterns similar to those observed in the *Sld27* mutant, although the magnitude of change was lower (Supplementary Table S11b).

Then, we examined tissue-preferential expression of the genes. *SlD27* and *SlCCD8* displayed strong root-preferential expression, with leaf-to-root RE ratios of 10^{-3} and 10^{-4}, respectively (Fig. 10b; Supplementary Table S11c). In contrast, *SlD27-LIKE1* and *SlD27-LIKE2* were predominantly expressed in leaves, showing leaf-to-root RE ratios of 10^{2} and 10^{1} under both P− and P+ conditions (Fig. 10b; Supplementary Table S11c and d). In Wt plants, the expression patterns of all four genes generally mirrored those observed in the *Sld27* mutant, with the exception of *SlCCD8*, which exhibited a lower leaf-to-root RE ratio (Supplementary Table S11e and f). Finally, we assessed whether any of the genes were differentially expressed in the *Sld27* mutant compared with the Wt plants. *SlCCD8* expression was higher in the mutant in both roots (∼1.8-fold) and leaves (∼7-fold). In contrast, *SlD27* expression in roots was reduced by ∼3.3-fold under P− and ∼5.3-fold under P+ conditions. *SlD27-LIKE2* showed a moderate increase in root expression under P− condition (∼1.35-fold) and a slight decrease in leaves under P+ (∼1.2-fold) condition (Fig. 10c; Supplementary Table S11g and h).

Discussion

Various tomato lines with either complete or partial inactivation of genes involved in SL biosynthesis have been previously generated using different strategies and genetic backgrounds (Cuccurullo et al. 2022), thus preventing direct comparisons of gene effects on parasitic plant resistance and on host plant phenotype. In this study, we successfully generated a complete panel of CRISPR/Cas9 KO lines targeting the core genes involved in SL biosynthesis (*SlD27*, *SlCCD7*, *SlCCD8*, and *SlMAX1*), all within the same cultivar, Ailsa Craig. Studying mutants in the same genetic background reduces genetic variability and interactions, making it easier to link observed traits directly to the mutation being studied. This leads to more accurate, reproducible results and helps identify the specific roles of genes, especially in complex traits like metabolism, development, or stress responses.

To assess the breeding potential of these novel alleles as sources of resistance to parasitic weeds, we evaluated the biochemical composition of the root exudates and their effects on the *in vitro* germination of two common broomrape species parasitizing tomato. An *in vivo* infection assay was included to validate the *in vitro* results. Additionally, we performed a comprehensive phenotypic characterization of the edited lines, with a particular focus on the biochemical profile of the fruits. Finally, we analyzed the expression of *SlD27*, *SlCCD8*, *SlD27-LIKE1*, and *SlD27-LIKE2* in leaf and root tissues of *Sld27*.

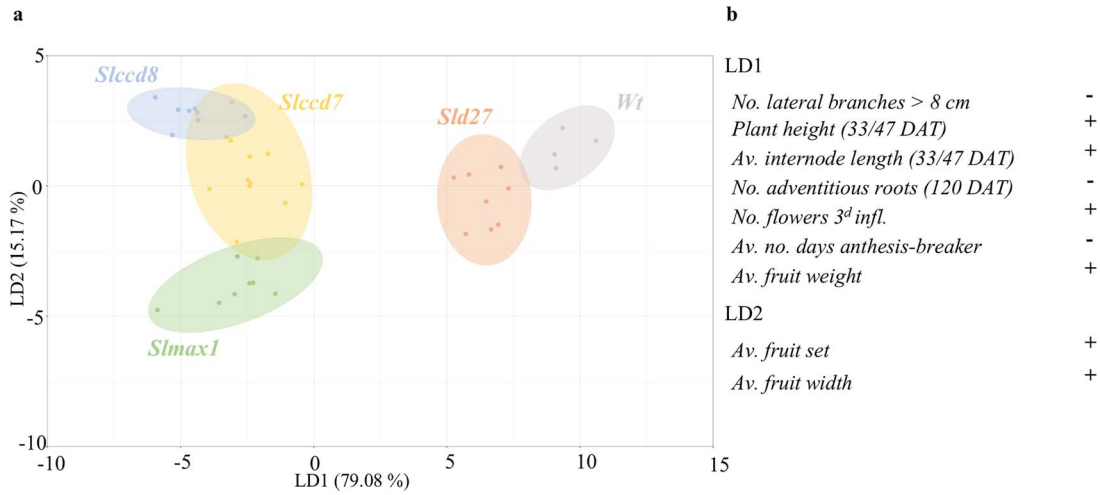

Figure 8. Bidimensional distribution of genotypes (ovals) and lines (dots) after linear discriminant analysis (LDA) of morphological, reproductive, and fruit-related traits. (a) Bidimensional distribution of scores assigned to CRISPR/Cas9 KO lines targeting SL biosynthesis genes: *Sld27* (*d27*-KO1, *d27*-KO2; orange), *Slccd7* (*ccd7*-KO1, *ccd7*-KO2, *ccd7*-KO3; yellow), *Slccd8* (*ccd8*-KO1, *ccd8*-KO2; blue), and *Slmax1* (*max1*-KO1, *max1*-KO2; green). The nonedited control genotype (wild-type, Wt) is represented in grey (for each line, $n = 4$). The two scores for each line were calculated using the linear discriminant functions LD1 (*x*-axis) and LD2 (*y*-axis), which together explain 94.25% of the observed variability. (b) Traits with strong correlation to LD1 and LD2 are highlighted (+: $r \geq 0.6$; −: $r \leq -0.6$). DAT: days after transplant.

The *Sld27* mutant shows a mild phenotype, likely due to the expression of *SlD27* paralogues

Notably, this study provides the first characterization of a *d27* loss-of-function mutant in a dicotyledonous crop species. The phenotypic variations observed in tomato *Sld27* lines are relatively mild compared with those reported for *d27* mutants in rice and *Arabidopsis* (Lin et al. 2009, Waters et al. 2012), although direct comparison across species can be complicated by the distinct molecular wirings involved in specific physiological processes (Uauy et al. 2025). In tomato, we have further extended the phenotypes associated with *d27* to include reproductive and fruit-related traits. To date, previous studies of *D27* have been limited to a small number of species, primarily *Arabidopsis*, rice, and the bryophyte *Marchantia polymorpha* (Lin et al. 2009, Waters et al. 2012, Jibran et al. 2024). Consistent with observations in rice and *Arabidopsis*, the *SlD27* gene is essential for SL biosynthesis in tomato, as orobanchol, solanacol, and didehydro-orobanchol fell below the detection limit in root exudates. In the rice *Osd27* mutant, 4-deoxyorobanchol was undetectable in root exudates, preventing the germination of *O. minor* seeds *in vitro* (Lin et al. 2009). In tomato, root exudates collected from *Sld27* lines determined a marked reduction in the seed germination of the parasitic plant species *P. ramosa*, *P. aegyptiaca*, and *O. minor*. This effect was accompanied by a strong inhibition of the parasitic shoot emergence *in vivo*, although the response was less pronounced than that observed for *Slccd7*. Likewise, root exudates from *Arabidopsis Atd27* reduced, but did not abolish, the germination rate of the parasitic weed *Striga hermonthica* (L.) (Yang et al. 2023).

The *D27* gene encodes an iron-containing isomerase that is conserved across higher plants and algae but absent in animals and fungi (Waters et al. 2012). Recent studies have identified *D27* paralogous genes (*D27-LIKE1* and *D27-LIKE2*), in rice (Liu et al. 2020) and *Arabidopsis* (Gulyás et al. 2022, Yang et al. 2023). Notably, the AtD27-LIKE1 isomerase contributed, albeit to a lesser extent, to SL biosynthesis in *Arabidopsis*, as its overexpression in the *Atd27* genetic background partially restored the Wt phenotype (Yang et al. 2023). Furthermore, Kobuna et al. (2025) reported additive phenotypic effects in *Arabidopsis* double (*Atd27* and *Atd27-like1*) and triple (*Atd27*, *Atd27-like1*, and *Atd27-like2*) mutants in *Arabidopsis*, highlighting functional overlap among these isomerases.

In tomato, the presence of *SlD27-LIKE* genes has been predicted through phylogenetic analysis, and their relative contribution to SL biosynthesis and shoot/root development, compared to *SlD27*, is currently under investigation (Cuccurullo et al. 2024).

The expression of SL biosynthetic genes is typically induced under inorganic phosphorous starvation (P−) (Umehara et al. 2010, Zhang et al. 2018). *SlD27-LIKE1* did not show induction; instead, its expression declined in roots while remaining stable in leaves. In *Arabidopsis*, phloem mobility of *AtSlD27-LIKE1* mRNA was detected (Yang et al. 2023), suggesting that root transcript levels in tomato may likewise be affected by long-distance transport, although the magnitude of this effect remains to be determined. Importantly, *SlD27-LIKE1* transcript abundance was comparable in Wt and *Sld27* mutant lines, indicating that its regulation may be largely independent of SL availability in tomato. In addition, the predicted plastid-targeting peptide in SlD27-LIKE1 suggests potential colocalization with early SL biosynthetic enzymes in tomato, consistent with observations in *Arabidopsis* (Gulyás et al. 2022, Yang et al. 2023).

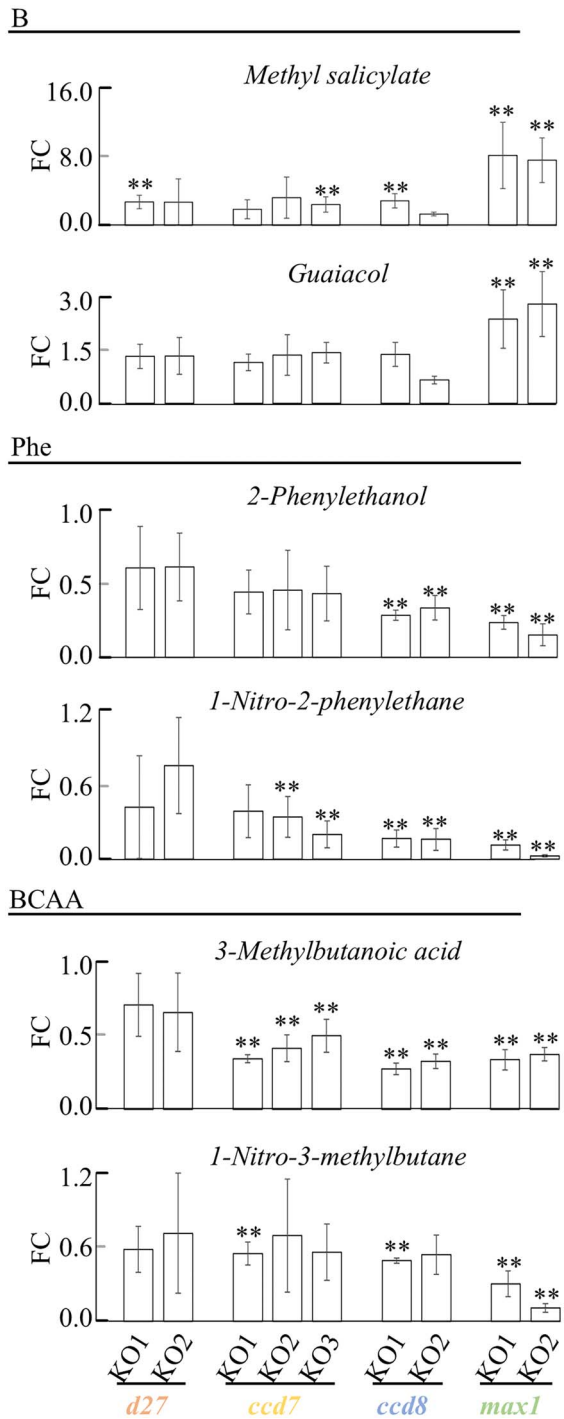

Figure 9. Alterations in key VOCs in fruits of CRISPR/Cas9 KO lines targeting SL biosynthesis genes. Bar charts display the mean fold changes (FCs) ± SD for the four genes relative to nonedited control plants (wild-type, Wt) ($n = 4$ for each KO line). Means statistically different from the Wt by Student's *t*-test are marked with asterisks: $P \leq 0.05$ (∗); $P \leq 0.01$(∗∗). VOCs are categorized by metabolic pathways (B: benzenoid/phenylpropanoid; BCAA: branched-chain amino acid–related; Phe: phenylalanine derivative).

In contrast, *SlD27-LIKE2* showed induction under P— and moderate responsiveness to SL levels. However, its subcellular localization remains unresolved. Although no experimental evidence currently supports plastid targeting of SlD27-LIKE2, such localization cannot be excluded, as several nuclear-encoded proteins lack a canonical transit peptide (Armbruster et al. 2009). Notably, phloem mobility of *AtD27-LIKE2* mRNA was predicted in *Arabidopsis* (Thieme et al. 2015).

The *Sld27* line was also characterized by reduced expression of the mutagenized *SlD27*, likely resulting from nonsense-mediated mRNA decay triggered by the presence of a premature termination codon (Lykke-Andersen and Jensen 2015). In addition, the elevated expression of *SlCCD8*, particularly in leaf, is consistent with feedback upregulation of the SL biosynthetic pathway, a response previously reported in SL mutant lines of tomato and *Arabidopsis* (Waters et al. 2012, Zhang et al. 2018).

Collectively, these findings, together with the preferential expression of *SlD27-LIKE1* in leaves, identify this gene as a strong candidate for sustaining localized SL biosynthesis in the shoot of *Sld27* mutants, thereby contributing to their mild phenotype. Although nonenzymatic isomerization of all-*trans*-β-carotene to 9-*cis*-β-carotene can occur under heat or light exposure, D27-LIKE1 is thought to maintain optimal physiological levels of 9-*cis*-β-carotene, particularly under conditions favouring uncontrolled *cis–trans* interconversion (Gulyás et al. 2022).

SLs are transported unidirectionally from root to shoot, where their detection remains challenging because concentrations are close to or below the analytical detection limit (Dun et al. 2023). This implies that SLs synthesized in the shoot are unlikely to support root exudation into the rhizosphere or contribute substantially to parasitic seed germination. Grafting experiments in tomato using wild-type scions combined with *Slccd7* and *Slccd8* rootstocks support this evidence (Dor et al. 2011, Karniel et al. 2024). Nevertheless, the *in vivo* infection assay suggests that the tomato *Sld27* mutant lines may still exude very low, yet analytically undetectable, amounts of SLs. The extent of phloem mobility of *SlD27-LIKE* transcripts, together with their potential contribution to root SL biosynthesis, may underline this residual activity, but further investigation is required.

Phenotypic changes, varying in both intensity and specificity, are influenced by disruptions at different points along the SL biosynthetic pathway

In contrast to the *Sld27* lines, the *Slccd7*, *Slccd8*, and *Slmax1* lines exhibited significant alterations in morphological, reproductive, and fruit-related traits. The *Slccd*s lines were notably characterized by an increased production of adventitious roots compared to the other lines. This trait has been previously documented in *ccd7* and *ccd8* lines from various species (Rasmussen et al. 2012, Liu et al. 2013). For instance, Kohlen et al. (2012) reported an elevated number of adventitious roots in the stems of *Slccd8* RNAi lines. This phenomenon is thought to be related to higher auxin concentrations and/or increased auxin sensitivity (Kohlen et al. 2012, Rasmussen et al. 2012). However, it remains intriguing to explore whether the extensive proliferation of HRs observed in the *Slccd7* and *Slccd8* lines is

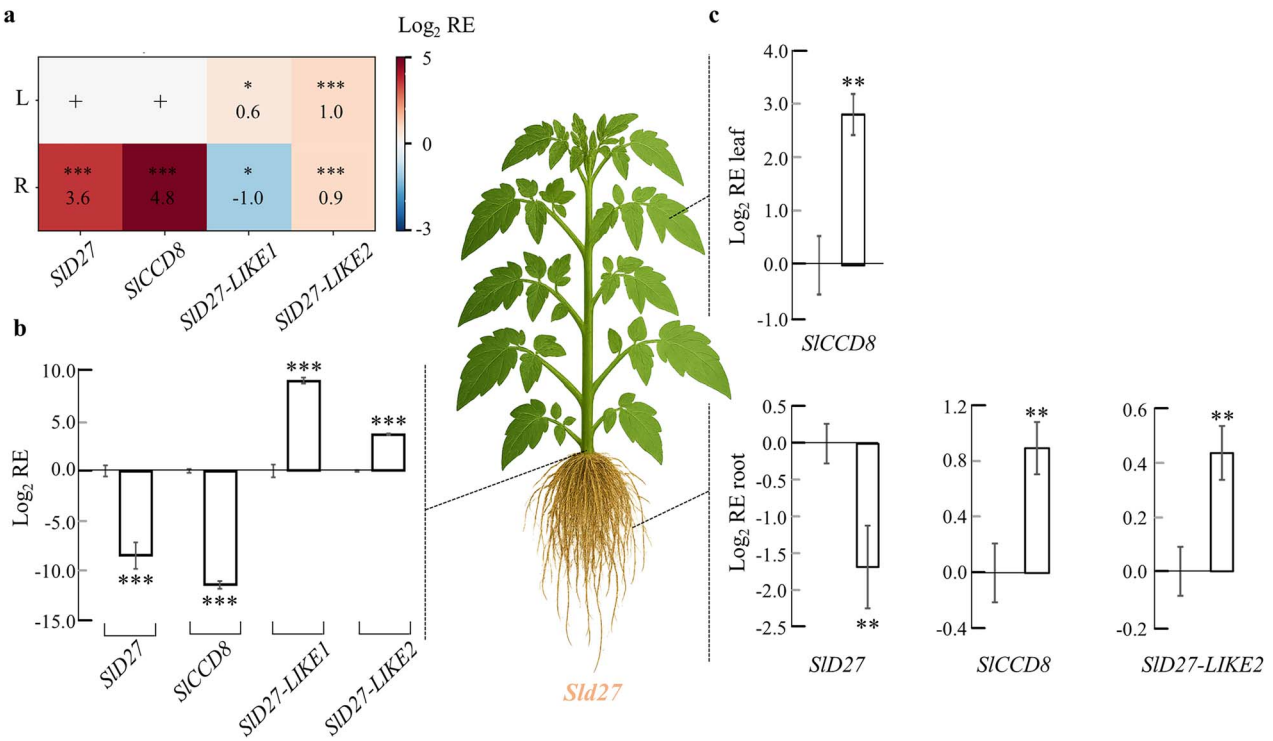

Figure 10. Expression analysis of *SlD27-LIKE1* and *SlD27-LIKE2* genes in the *Sld27* mutant line. (a) Relative expression (RE, $\log_2$) of the *SlD27-LIKE* genes, together with the canonical *SlD27* and the *SlCCD8* genes, in leaf (L) and root (R) tissue of the CRISPR/Cas9 KO line *Sld27* (*d27-KO1*) under low inorganic phosphate (P−) condition. Expression in both leaves and roots under normal phosphate (P+) was set to $\log_2 1$, except for *SlD27* and *SlCCD8*, which were undetectable under P+; in these cases, the RE could not be determinate and a '+' indicates expression only under P−. (b) Relative expression (RE, $\log_2$) of the *SlD27-LIKE*, *SlD27*, and *SlCCD8* genes in the leaf tissue of the *Sld27* mutant line with root expression set to $\log_2 1$. (c) RE ($\log_2$) of the genes differentially expressed in leaf and root of the *Sld27* under P−. The expression level of nonedited wild-type (Wt) control plants was set to $\log_2 1$. Each line was analysed in three independent biological replicates ($n = 3$). The housekeeping genes *Solyc01g056940* (*Ubiquitin*) and *Solyc11g150146* (*Elongation factor 1*) were the two used to normalize the expression of the four target genes. Error bars represent means ± SD. Significant differences were determined by Student's *t*-test and they are indicated with asterisks: $P \leq 0.001$ (***); $P \leq 0.01$ (**); $P \leq 0.05$ (*).Differences in gene expression that are not significant are reported in Supplementary Table S11. Note: the tomato plant image was generated using Microsoft Copilot 2026 with the prompt 'Create an image of a tomato plant without soil, showing naked roots and no fruits' (https://copilot.microsoft.com/).

also linked to the absence of additional specific apocarotenoids produced by these two CCDs.

The *Slmax1* lines, edited in the downstream gene of the SL biosynthetic pathway, exhibited unique phenotypes not previously reported or specifically associated (Zhang et al. 2018, Bari et al. 2021a), with this genotype.

Slmax1 lines retained a significant germination percentage for *P. ramosa* and for the nonhost species *O. minor*. The latter differs from *Phelipanche* spp. because it is not characterized by spontaneous germination, and it seems to be specifically sensitive to SLs (Takei et al. 2023) and not to other germination inducers (i.e. isothiocyanates). Therefore, a possible explanation for this discrepancy may lie in the accumulation of carlactone in the *Slmax1* lines. In *Arabidopsis*, carlactone exhibits SL-like activity and has a clear stimulating effect on *S. hermonthica* seed germination (Alder et al. 2012). Although carlactone has been proposed as the possible mobile signal in plants (Al-Babili and Bouwmeester 2015, Dun et al. 2023), it has not been detected in root exudates but only in root extracts of rice and *Arabidopsis* (Seto et al. 2014). It is important to note that in a *Slmax1* TILLING mutant, trace levels of SLs were still detectable in both root exudates and root extracts. However, no germination assay was performed to assess whether these small amounts of SLs were sufficient to induce broomrape germination (Zhang et al. 2018). It remains unclear whether *Slmax1* releases unknown compound(s) and/or precursor(s) capable of inducing germination of root parasitic weeds. Under our experimental conditions, however, we were unable to detect any candidate precursor(s), including carlactone, possibly due to their low abundance or limitations in analytical sensitivity.

The *Slmax1* lines were also characterized by a dramatic reduction in fruit set and by a consistent increase in the time from anthesis to the onset of ripening (breaker); these traits were accompanied by the phenotypes already observed in the *Slccd*s lines (reduction in number of flowers and fruit weight/-size). General reproductive defects in the *Slmax1* genotype have been previously reported (Zhang et al. 2018), as well as reductions in flower and/or fruit size associated with alteration

in SL content in *Slccd8* lines (Kohlen et al. 2012, Bari et al. 2019). While the role of SLs in flowering (i.e. induction, number of flowers, and inflorescence size) has been extensively studied in tomato and other species, with a recent model proposed (Visentin et al. 2024 and references therein), the role of SLs in fruit set and ripening remains less understood. In strawberry, the expression of the two *MAX1* orthologues was high in style before and after pollination, compared to the lower expression of the *CCD7* orthologue and the negligible expression of the *D27* and *CCD8* orthologues (Wu et al. 2019). These findings align with our observations, highlighting a significant contribution of *SlMAX1* to fruit set. This suggests the intriguing possibility of a specific additive effect of the *SlMAX1* loss of function in combination with alteration in SL content. Additionally, it is plausible that the reproductive and fruit phenotypes observed in *Slccd*s and S*lmax1* lines are linked to the coregulation of SLs and auxin sensitivity and/or transport (Kohlen et al. 2012, Mashiguchi et al. 2021). However, the extent of this regulation in fleshy fruits warrants further investigation, and the impact of photosynthate redistribution in highly branched phenotypes cannot be excluded.

CCDs and MAX1 impact the production of VOCs during fruit ripening

Despite the observed phenotypes in *Slccd*s and *Slmax1* lines, the carotenoid, sugar, and flavonoid content in the fruits did not differ significantly from the control. Additionally, water loss, an important determinant of changes in fruit firmness during ripening (Gidado et al. 2024), remained unaltered (Supplementary Table S4). While these results were not surprising for the *Sld27* lines, given their mild phenotype, they were unexpected for the lines with more pronounced pleiotropic effects, such as *Slccd*s or *Slmax1*. Interestingly, previous studies reported high expression of *SlCCD7* in tomato fruit at the immature green stage (Vogel et al. 2010) and of *CCD7* and *CCD8* in young kiwi fruit (Ledger et al. 2010).

To explore potential variations in tomato fruit ripening that may have been overlooked, we analyzed VOCs in fruits from our panel of CRISPR/Cas9-edited tomato lines. In addition to their significance as breeding traits for fruit quality, VOCs, deriving from a diversity of metabolic pathways, served as important metabolic checkpoints for possible direct or indirect effects of SLs.

The fruits of *Slmax1* lines showed a significant and consistent accumulation of MeSA and guaiacol. MeSA is derived from the methylation of the phytohormone salicylic acid (SA) and acts as a transduction signal in systemic acquired resistance. In tomato fruit, MeSA concentration typically peaks at 15 days after pollination, then declines and remains constant during ripening. As a volatile compound, it is generally associated with a wintergreen flavour, which is often negatively perceived by consumers (Tieman et al. 2010, Frick et al. 2023, Kaur et al. 2023).

Similarly, guaiacol is synthesized from SA (Mageroy et al. 2012, Zhou et al. 2021). Guaiacol contributes to a 'smoky' or 'medicinal' flavour and is prominently emitted in tomato fruits at the mature green stage in both 'smoky' and 'nonsmoky' varieties, although its levels drop dramatically in nonsmoky varieties after the breaker stage (Tikunov et al. 2013). It is often negatively perceived by consumers (Kaur et al. 2023) and the tomato variety used in this work belongs to the 'smoky' group, with a high production of guaiacol in the ripe fruit.

In general, changes in in the B pathway can be determined by external causes, such as biotic stress or plant treatments (Huang et al. 2020), which could not be excluded in our lines. However, in *Arabidopsis*, Kusajima et al. (2022) demonstrated that the *max4* mutant (*Slccd8* homologue) exhibited higher free SA levels in leaves compared to the *max3* mutant (the *Slccd7* homologue), which exhibited similar SA levels to the control. This suggests that the perturbation of SA homeostasis may increase with further disruption of the SL biosynthetic pathway.

Amino acid–derived VOCs are key contributors to tomato aroma and flavour, forming during the ripening process (Kaur et al. 2023). Consistently with a normal ripening process, the two immediate downstream aldehydes of the amino acid phenylalanine (2-phenylacetaldehyde; floral flavour; Phe) and leucine (3-methylbutanal; malty, earthy flavour; BCAA), both positively contributing to the flavour, were unaltered in our edited lines. In contrast, several downstream VOCs positively contributing to flavour and derived from phenylalanine (2-phenylethanol: nutty, fruity flavour; 1-nitro-2-phenylethane: musty, earthy flavour; Phe) and leucine (1-nitro-3-methylbutane; 3-methylbutanenitrile; BCAA) were dramatically reduced by SL manipulation. Interestingly, we did not observe large variations in the production of VOCs belonging to the ApoC and L pathways, the two more interconnected to carotenoids (Kaur et al. 2023).

Considering the few VOCs altered in the *Sld27* lines, it is likely that the activity of CCD7, CCD8, and MAX1 directly or indirectly influences the ripening-associated biosynthesis of specific VOCs, thereby potentially affecting tomato flavour. The investigation of SLs' roles in the ripening processes of both climacteric and nonclimacteric species remains an underexplored but compelling area of research (Ferrero et al. 2018, Li et al., 2023b, Li et al. 2024) and our results contribute valuable insights into these dynamics.

Field use of tomato lines altered in SL biosynthesis

Based on morphophysiological characterization and resistance phenotype, the *SlD27* gene represents a promising breeding target for developing parasitic plant resistance in tomato. The mild phenotype observed in the *Sld27* lines appeared to be sufficient to sustain normal flowering and fruit development; additionally, preliminary results did not show yield penalties in controlled conditions (not shown). However, these results require further validation in different genetic backgrounds and under a broader range of physiological conditions (e.g. abiotic/biotic stress resistance) due to potential overlaps of carotenoid isomerases with other hormonal pathways (e.g. abscisic acid) (Tolnai et al. 2024, Ye et al. 2024).

Field trials are essential to evaluate yield performance comprehensively and the genetic materials developed in this study provide a unique platform for in-depth exploration of SL biosynthesis in a model crop of critical agriculture importance, such as tomato. These resources will be further enriched in the future by incorporating additional CRISPR/Cas9-edited genes involved in the biosynthesis and transport of SLs. The resulting edited plants have the potential to be used not only in field trials as complete specimens but also as rootstock for commercial cultivars/hybrids. Notably, recent field trials with tomato mutants have demonstrated the effectiveness of *Slccd7* and *Slccd8* rootstock in controlling *P. aegyptiaca* without yield losses or any apparent pleiotropic effect under normal growing conditions (Karniel et al. 2024). In our hands, preliminary results from field experiments using wild-type tomato scions grafted onto *Sld27* and *Slccd7* rootstocks support these findings (Nicolia et al. unpublished results).

However, the use of specific genotypes (e.g. *Slccd7*) as rootstock may also influence physiological traits, such as drought recovery and flowering (Visentin et al. 2020, 2024). Additionally, while the use of grafting has shown documented benefits for yield and quality improvement (Caradonia et al. 2023, Parisi et al. 2023), its adoption in open-field cultivation systems, particularly for processed tomato production, by contrast with fresh market tomato under protected culture, remains constrained due to the higher cost of grafted plants. This underscores the appeal of precise genetic modification (e.g. *SlD27*) in elite hybrid cultivars as a cost-effective and scalable solution for integrating SL-related resistance traits into commercial production systems.

Materials and Methods

Generation of CRISPR/Cas9 knockout plants

The design of the sgRNAs and the prediction of off-targets for the *SlD27*, *SlCCD7*, *SlCCD8*, and *SlMAX1* genes were performed with the software CRISPR-P 2.0 (Liu et al. 2017). CRISPR/Cas9 vector assembly was performed via the Golden Gate Cloning method (Engler et al. 2014). Vector efficiency was preliminary assessed in tomato HRs (Ron et al. 2014). The four validated vectors were independently introduced into *A. tumefaciens* strain EHA105. Transformation of tomato cotyledons (*S. lycopersicum* L. cv. *Ailsa Craig*) was carried out following the protocol by Qiu et al. (2007). At least two independent KO lines per gene, each showing an out-of-frame insertion in the coding sequence, were selected and advanced to the T_2 generation through self-pollination. All the PCR primers used are listed in the Supplementary Table S12.

Parasitic weed germination and *in vivo* infection assays

Tomato plants were grown in pots (three to four biological replicates per genotype) filled with vermiculites under a 16-h light (~240 μmol m^{-2} s^{-1}) and 8-h dark cycle at 23–25°C. To collect root exudates containing SLs, tap water (100–200 mL) was poured onto the soil surface, and the drained solutions containing root exudates were collected. These solutions were extracted with ethyl acetate, and the ethyl acetate phase was subsequently dried over anhydrous $MgSO_4$ and concentrated *in vacuo*. All the crude samples were stored at 4°C until use. These root exudate samples were used for both germination assay and LC–MS/MS analysis. Germination assays with broomrape seeds were conducted as reported previously (Yoneyama et al. 2007). Seed germination was assessed by counting seeds where the radicle had protruded through the seed coat.

Tomato plants (10 plants per plot, with 3 biological replicates per line) were grown in plastic trays containing peat mixed with *P. ramosa* (L.) seeds. Plants were grown in a phytotron, and the cumulative number of emerged *P. ramosa* shoots was recorded for each plot and line.

LC–MS/MS analysis of root exudates

Tomato SLs were analyzed using ultra-performance liquid chromatography coupled with tandem mass spectrometry (UPLC–MS/MS) following the protocol described by Yoneyama et al. (2022). The analysis was performed on an Acquity UPLC System (Waters, Milford, MA, USA) connected to a Xevo TQD triple-quadrupole mass spectrometer (Waters Milford, MA, USA) with an electrospray ionization interface. Multiple reaction monitoring (MRM) transitions were used to detect specific SLs.

Detection of plant morphological, reproductive, and fruit-related traits

Four biological replicates for each of the T_2 tomato biallelic homozygous edited lines *Sld27* (*d27*-KO1, *d27*-KO2), *Slccd7* (*ccd7*-KO1, *ccd7*-KO2, and *ccd7*-KO3), *Slccd8* (*ccd8*-KO1, *ccd8*-KO2, and *ccd8*-KO3), and *Slmax1* (*max1*-KO1 and *max1*-KO2), as well as nonedited control plants, were transplanted into pots containing a mixture of peat and perlite. These plants were grown in a phytotron under regular watering and fertilizing conditions, with the pots arranged in a randomized design. The morphological, reproductive, and fruit-related traits were recorded at specific DAT. Ten fruits per biological replicate were tagged at the breaker stage. Fruits were harvested after 7 days (breaker +7), measured, and subsequently used for biochemical analysis. Five additional fruits per biological replicate were harvested at the mature green stage and stored in a controlled environment to estimate water loss. The number of adventitious roots was counted on plants at 120 DAT.

Extraction and U/HPLC-PDA analysis of chlorogenic acid, rutin, naringenin, and sugars

Each biological replicate was analyzed in duplicate for simple sugars (fructose and glucose) for the two flavonoids NaCh and Rut, and the phenol CA. The CA and the NaCh and Rut were extracted following a previously described method (de Vos et al. 2007), with minor modifications. The analyses were performed using an Ultimate 3000 Ultra Performance Liquid Chromatography (UPLC) system (Thermo Fisher Scientific, Sunnyvale, CA, USA). The extraction of simple sugars was performed on 250 mg of lyophilized powder and the extract was subjected to analysis on the E-Alliance High-Performance Liquid Chromatography (HPLC) system (Waters, Milford, MA, USA), with data acquired and analyzed using Waters Empower software. Peak areas for CA, NACh, Rut, and sugars were recorded using authentic, distinct, and appropriately diluted standards (Sigma-Aldrich, Saint Louis, MO, USA). Finally, the compound content was expressed as fold change relative to the nonedited control plants.

Extraction and HPLC-PDA analysis of carotenoids and tocopherols

Carotenoids and tocopherols were extracted following the protocols described by Barja et al. (2021) and Ezquerro et al. (2023) with modifications. Liquid chromatography was performed using an HPLC Water Alliance 2695 Separations module, with carotenoids detected by a Waters 996 PDA detector and tocopherols identified using a Waters 2475 Multi λ fluorescence detector. Peak areas were recorded and analyzed using Waters Millennium software (Waters, Milford, MA, USA). The areas were normalized by an internal standard, and carotenoid and tocopherol content was expressed as fold change relative to the nonedited control plants.

Extraction and gas chromatography coupled with mass spectrometry analysis of volatile organic compounds

VOCs were extracted and analyzed as reported in Rambla et al. (2017). For the analysis, 500 mg of fresh pericarp powder, obtained from the five pooled fruits per biological replicate and stored at −80°C, were used. VOCs were captured using headspace solid-phase microextraction and subsequently separated and identified by gas chromatography coupled with mass spectrometry. VOCs from the headspace were extracted using a 65-μm Polydimethylsiloxane/divinylbenzene (PDMS/DVB) solid-phase microextraction fibre (Supelco–Merck, Darmstadt, Germany). Desorption of the compounds from the fibre occurred at the injection port of a 6890N gas chromatograph (Agilent Technologies, Santa Clara, CA, USA). Data acquisition was performed using a 5975B mass spectrometer (Agilent Technologies, Santa Clara, CA, USA). Compound identification was accomplished by comparing retention times and mass spectra with those of pure standards. Peak areas were recorded and normalized results were expressed as the ratio of compound abundance in each sample relative to the reference admixture.

Gene expression analysis

Total RNA was extracted from leaves and roots of the nonedited Wt control plants and CRISPR/Cas9 KO lines *Sld27* (*d27*-KO1) using the RNAeasy Mini Kit (Qiagen, Hilden, Germany). For each sample, 300 ng of RNA was used to synthesize cDNA with the RevertAid First Strand cDNA Synthesis Kit (Thermo Fisher Scientific, Sunnyvale, CA, USA) following the manufacturer's instructions. Quantitative real-time PCR was performed on a QuantStudio™ 6 Pro system using PowerTrack™ SYBR™ Green Master Mix chemistry, according to the manufacturer's protocol (Thermo Fisher Scientific, Sunnyvale, CA, USA). Primer sequences are listed in Supplementary Table S12.

Statistical analysis

Statistical analysis was performed using single factor ANOVA and Tukey's HSD with the Real Statistic software package (https://real-statistics.com/). Statistical analysis on VOCs and gene expression was performed by a *t*-test with the software Office 365 Excel (Redmond, WA, USA). Linear discriminant analysis (LDA) was conducted using the MASS package in R (https://cran.r-project.org/web/packages/MASS/index.html).

Acknowledgments

The authors wish to thank Maurizio Vurro and Angela Boari (CNR, Institute of Sciences of Food Production, Bari, Italy) for their valuable assistance with parasitic weed manipulation. They are grateful to Andrea Mazzucato (University of Tuscia, Viterbo, Italy) and Gianfranco Diretto (ENEA-Casaccia, Rome, Italy) for their guidance on plant phenotypic analysis. Special thanks to Giuseppe Mennella for his advice on metabolic analysis and to Accursio Venezia and Mario Parisi for their support with phytotron and plant management (CREA, Research Centre for Vegetable and Ornamental Crops, Pontecagnano, Italy). The authors also appreciate Andrea Burato, Giovanna Forte, Francesco Vitale, and Mario Salzano for their help with plant handling and tomato sampling (CREA, Research Centre for Vegetable and Ornamental Crops, Pontecagnano, Italy). The authors are grateful to Nutcha Manichart for his support on germination assay with parasitic plants. The authors acknowledge Teresa Caballero Vizcaíno, Ana Espinosa Ruiz, and the Plant Metabolomics lab of the IBMCP (Valencia, Spain) for their technical support in plant metabolomics. Finally, the authors thank Luigi Cattivelli (CREA, Research Centre for Genomic and Bioinformatic, Fiorenzuola D'Arda, Italy) for coordinating the project BIOTECH and his valuable advice.

Author Contributions

A.N., N.D.A., and T.C. conceived the experiments. F.Ca., A.C., and F.Co. assembled the vectors and carried out *in silico* analysis. A.N., A.C., and G.Fe. carried out the *in vitro* experiments. A.N. and A.C. carried out phenotypic analysis in the phytotron. G.Fr. and A.D.A. did the metabolic analysis on sugars and flavonoids. A.N., L.P., and J.L.R. carried out metabolic analysis on carotenoids and VOCs. A.N., A.C., G.Fr., M.M.R., J.L.R., and A.G. analyzed metabolic data and revised results. K.T. and K.Y. carried out strigolactone analysis on root exudates and performed the germination assay. A.N. and A.C. carried out the *in vivo* infection assay and the gene expression analysis. A.N., A.C., N.D.A., and T.C. wrote the manuscript. All the authors revised and approved the manuscript.

Supplementary Data

Supplementary data is available at *PCP* online.

Conflict of Interest

None declared.

Funding

The work presented here was financially supported by the Italian Ministry of Agriculture, Food Sovereignty and Forests (MASAF), project BIOTECH subproject Cisget (DM 15924, 18-05-2018). J.L.R. acknowledges funding from the Spanish Ministry of Science and Innovation by a Juan de la Cierva-incorporación grant (IJC2020-045612-I). A.G. acknowledges funding from the Spanish Ministry for PGC project PID2022-141438OB-I00 and to the EU for Harnesstom contract 101000716. K.Y. was supported by the Japan Science and Technology Agency (FOREST, JPMJFR220F).

Data Availability

The Sanger sequences of target and off-target sites for the *Sld27*, *Slccd7*, *Slccd8*, and *Slmax1* lines, including the nonedited control plant, are available at Mendeley Data repository (https://doi.org/10.17632/7vwj6cz972.1).

References

Al-Babili, S. and Bouwmeester, H.J. (2015) Strigolactones, a novel carotenoid-derived plant hormone. *Annu. Rev. Plant Biol.* 66: 161–186. https://doi.org/10.1146/annurev-arplant-043014-114759.

Alder, A., Jamil, M., Marzorati, M., Bruno, M., Vermathen, M., Bigler, P., et al. (2012, 1979) The path from β-carotene to carlactone, a strigolactone-like plant hormone. *Science* 335: 1348–1351. https://doi.org/10.1126/science.1218094.

Arcieri, F., Giudice, G., Guerriero, M., Delvento, C., Schilder, M., Giancaspro, A., et al. (2025) Field resistance to *Orobanche crenata* in pea (*Pisum sativum* L.): beyond strigolactones. *BMC Plant Biol.* 25:1 25: 1–11. https://doi.org/10.1186/S12870-025-07296-X.

Armbruster, U., Hertle, A., Makarenko, E., Zühlke, J., Pribil, M., Dietzmann, A., et al. (2009) Chloroplast proteins without cleavable transit peptides: rare exceptions or a major constituent of the chloroplast proteome? *Mol. Plant* 2: 1325–1335. https://doi.org/10.1093/mp/ssp082.

Ban, X., Qin, L., Yan, J., Wu, J., Li, Q., Su, X., et al. (2025) Manipulation of a strigolactone transporter in tomato confers resistance to the parasitic weed broomrape. *Innovation* 6: 100815. https://doi.org/10.1016/j.xinn.2025.100815.

Bari, V.K., Nassar, J.A. and Aly, R. (2021a) CRISPR/Cas9 mediated mutagenesis of MORE AXILLARY GROWTH 1 in tomato confers resistance to root parasitic weed Phelipanche aegyptiaca. *Sci. Rep.* 11: 3905. https://doi.org/10.1038/s41598-021-82897-8.

Bari, V.K., Nassar, J.A., Kheredin, S.M., Gal-On, A., Ron, M., Britt, A., et al. (2019) CRISPR/Cas9-mediated mutagenesis of CAROTENOID CLEAVAGE DIOXYGENASE 8 in tomato provides resistance against the parasitic weed *Phelipanche aegyptiaca*. *Sci. Rep.* 9: 11438. https://doi.org/10.1038/s41598-019-47893-z.

Bari, V.K., Nassar, J.A., Meir, A. and Aly, R. (2021b) Targeted mutagenesis of two homologous ATP-binding cassette subfamily G (ABCG) genes in tomato confers resistance to parasitic weed *Phelipanche aegyptiaca*. *J. Plant Res.* 134: 585–597. https://doi.org/10.1007/s10265-021-01275-7.

Barja, M.V., Ezquerro, M., Beretta, S., Diretto, G., Florez-Sarasa, I., Feixes, E., et al. (2021) Several geranylgeranyl diphosphate synthase isoforms supply metabolic substrates for carotenoid biosynthesis in tomato. *New Phytol.* 231: 255–272. https://doi.org/10.1111/nph.17283.

Bouwmeester, H., Li, C., Thiombiano, B., Rahimi, M. and Dong, L. (2021) Adaptation of the parasitic plant lifecycle: germination is controlled by essential host signaling molecules. *Plant Physiol.* 185: 1292–1308. https://doi.org/10.1093/plphys/kiaa066.

Brun, G., Spallek, T., Simier, P. and Delavault, P. (2021) Molecular actors of seed germination and haustoriogenesis in parasitic weeds. *Plant Physiol.* 185: 1270–1281. https://doi.org/10.1093/plphys/kiaa041.

Caradonia, F., Francia, E., Alfano, V. and Ronga, D. (2023) Grafting and plant density influence tomato production in organic farming system. *Horticulturae* 9: 669. https://doi.org/10.3390/horticulturae9060669.

Chachalis, D., Tani, E., Kapazoglou, A., Gerakari, M., Petraki, A., Pérez-Alfocea, F., et al. (2025) Broomrapes in Major Mediterranean crops: from management strategies to novel approaches for next-generation control. *BioTech* 14: 40. https://doi.org/10.3390/biotech14020040.

Cuccurullo, A., D'Agostino, N., Rigano, M.M. and Nicolia, A. 2024. Editing the Dwarf27 (*D27*) gene family member to uncover their role in tomato plant physiology and development. In *Proceedings of the LXVII SIGA Annual Congress*. Bologna. ISBN: 978-88-944843-5-9

Cuccurullo, A., Nicolia, A. and Cardi, T. (2022) Resistance against broomrapes (*Orobanche* and *Phelipanche* spp.) in vegetables: a comprehensive view on classical and innovative breeding efforts. *Euphytica* 218: 82. https://doi.org/10.1007/s10681-022-03035-7.

de Vos, R.C., Moco, S., Lommen, A., Keurentjes, J.J., Bino, R.J. and Hall, R.D. (2007) Untargeted large-scale plant metabolomics using liquid chromatography coupled to mass spectrometry. *Nat. Protoc.* 2: 778–791. https://doi.org/10.1038/nprot.2007.95.

Dor, E., Yoneyama, K., Wininger, S., Kapulnik, Y., Yoneyama, K., Koltai, H., et al. (2011) Strigolactone deficiency confers resistance in tomato line SL-ORT1 to the parasitic weeds *Phelipanche* and *Orobanche* spp. *Phytopathology* 101: 213–222. https://doi.org/10.1094/PHYTO-07-10-0184.

Dun, E.A., Brewer, P.B., Gillam, E.M.J. and Beveridge, C.A. (2023) Strigolactones and shoot branching: what is the real hormone and how does it work? *Plant Cell Physiol.* 64: 967–983. https://doi.org/10.1093/pcp/pcad088.

Engler, C., Youles, M., Gruetzner, R., Ehnert, T.M., Werner, S., Jones, J.D.G., et al. (2014) A golden gate modular cloning toolbox for plants. *ACS Synth. Biol.* 3: 839–843. https://doi.org/10.1021/sb4001504.

Ezquerro, M., Li, C., Pérez-Pérez, J., Burbano-Erazo, E., Barja, M.V., Wang, Y., et al. (2023) Tomato geranylgeranyl diphosphate synthase isoform 1 is involved in the stress-triggered production of diterpenes in leaves and strigolactones in roots. *New Phytol.* 239: 2292–2306. https://doi.org/10.1111/nph.19109.

Fernández-Aparicio, M., Reboud, X. and Gibot-Leclerc, S. (2016) Broomrape weeds. Underground mechanisms of parasitism and associated strategies for their control: a review. *Front. Plant Sci.* 7: 135. https://doi.org/10.3389/fpls.2016.00135.

Ferrero, M., Pagliarani, C., Novák, O., Ferrandino, A., Cardinale, F., Visentin, I., et al. (2018) Exogenous strigolactone interacts with abscisic acid-mediated accumulation of anthocyanins in grapevine berries. *J. Exp. Bot.* 69: 2391–2401. https://doi.org/10.1093/JXB/ERY033.

Frick, E.M., Sapkota, M., Pereira, L., Wang, Y., Hermanns, A., Giovannoni, J.J., et al. (2023) A family of methyl esterases converts methyl salicylate to salicylic acid in ripening tomato fruit. *Plant Physiol.* 191: 110–124. https://doi.org/10.1093/PLPHYS/KIAC509.

Gidado, M.J., Gunny, A.A.N., Gopinath, S.C.B., Ali, A., Wongs-Aree, C. and Salleh, N.H.M. (2024) Challenges of postharvest water loss in fruits: mechanisms, influencing factors, and effective control strategies – a comprehensive review. *J. Agric. Food Res.* 17: 101249. https://doi.org/10.1016/J.JAFR.2024.101249.

Gobena, D., Shimels, M., Rich, P.J., Ruyter-Spira, C., Bouwmeester, H., Kanuganti, S., et al. (2017) Mutation in sorghum LOW GERMINATION STIMULANT 1 alters strigolactones and causes *Striga* resistance. *Proc. Natl. Acad. Sci. USA* 114: 4471–4476. https://doi.org/10.1073/pnas.1618965114.

Gulyás, Z., Moncsek, B., Hamow, K.Á., Stráner, P., Tolnai, Z., Badics, E., et al. (2022) D27-LIKE1 isomerase has a preference towards *trans*/*cis* and *cis*/*cis* conversions of carotenoids in *Arabidopsis*. *Plant J.* 112: 1377–1395. https://doi.org/10.1111/TPJ.16017.

Huang, W., Wang, Y., Li, X. and Zhang, Y. (2020) Biosynthesis and regulation of salicylic acid and *N*-hydroxypipecolic acid in plant immunity. *Mol. Plant* 13: 31–41. https://doi.org/10.1016/J.MOLP.2019.12.008.

Jamil, M., Margueritte, O., Yonli, D., Wang, J.Y., Navangi, L., Mudavadi, P., et al. (2024) Evaluation of granular formulated strigolactone analogs for *Striga* suicidal germination. *Pest Manag. Sci.* 80: 4314–4321. https://doi.org/10.1002/ps.8136.

Jibran, R., Tahir, J., Andre, C.M., Janssen, B.J., Drummond, R.S.M., Albert, N.W., et al. (2024) DWARF27 and CAROTENOID CLEAVAGE DIOXYGENASE 7 genes regulate release, germination and growth of gemma in *Marchantia polymorpha*. *Front. Plant Sci.* 15: 1358745. https://doi.org/10.3389/fpls.2024.1358745.

Karniel, U., Koch, A., Bar Nun, N., Zamir, D. and Hirschberg, J. (2024) Tomato mutants reveal root and shoot strigolactone involvement in branching and broomrape resistance. *Plants* 13: 1554. https://doi.org/10.3390/plants13111554.

Kaur, G., Abugu, M. and Tieman, D. (2023) The dissection of tomato flavor: biochemistry, genetics, and omics. *Front. Plant Sci.* 14: 1144113. https://doi.org/10.3389/fpls.2023.1144113.

Kobuna, H., Kanno, Y., Fukuhara, D., Seto, Y., Kushiro, T. and Okamoto, M. (2025) Genetic analysis of β-carotene isomerase in *Arabidopsis thaliana*. *Biochem. Biophys. Res. Commun.* 776: 152185. https://doi.org/10.1016/J.BBRC.2025.152185.

Kohlen, W., Charnikhova, T., Lammers, M., Pollina, T., Tóth, P., Haider, I., et al. (2012) The tomato carotenoid cleavage dioxygenase8

(SlCCD8) regulates rhizosphere signaling, plant architecture and affects reproductive development through strigolactone biosynthesis. *New Phytol.* 196: 535–547. https://doi.org/10.1111/j.1469-8137.2012.04265.x.

Kusajima, M., Fujita, M., Soudthedlath, K., Nakamura, H., Yoneyama, K., Nomura, T., et al. (2022, 2022) Strigolactones modulate salicylic acid-mediated disease resistance in *Arabidopsis thaliana*. *Int. J. Mol. Sci.* 23: 5246. https://doi.org/10.3390/IJMS23095246.

Ledger, S.E., Janssen, B.J., Karunairetnam, S., Wang, T. and Snowden, K.C. (2010) Modified *CAROTENOID CLEAVAGE DIOXYGENASE8* expression correlates with altered branching in kiwifruit (*Actinidia chinensis*). *New Phytol.* 188: 803–813. https://doi.org/10.1111/j.1469-8137.2010.03394.x.

Li, C., Dong, L., Durairaj, J., Guan, J.-C., Yoshimura, M., Quinodoz, P., et al. (2023a) Maize resistance to witchweed through changes in strigolactone biosynthesis. *Science* 379: 94–99. https://doi.org/10.1126/science.abq4775.

Li, M., Yang, M., Liu, X., Hou, G., Jiang, Y., She, M., et al. (2023b) Pre-harvest application of strigolactone (GR24) accelerates strawberry ripening and improves fruit quality. *Agronomy* 13: 2699. https://doi.org/10.3390/agronomy13112699.

Li, M., Li, X., Du, J., Li, W., He, R., Lin, Y., et al. (2024) Effects of exogenous application of the strigolactone GR24 on quality and flavor components during postharvest storage of celery. *Postharvest Biol. Technol.* 212: 112900. https://doi.org/10.1016/J.POSTHARVBIO.2024.112900.

Lin, H., Wang, R.X., Qian, Q., Yan, M.X., Meng, X.B., Fu, Z.M., et al. (2009) DWARF27, an iron-containing protein required for the biosynthesis of strigolactones, regulates Rice tiller bud outgrowth. *Plant Cell* 21: 1512–1525. https://doi.org/10.1105/tpc.109.065987.

Liu, H., Ding, Y., Zhou, Y., Jin, W., Xie, K. and Chen, L.-L. (2017) CRISPR-P 2.0: an improved CRISPR-Cas9 tool for genome editing in plants. *Mol. Plant* 10: 530–532. https://doi.org/10.1016/j.molp.2017.01.003.

Liu, J., Novero, M., Charnikhova, T., Ferrandino, A., Schubert, A., Ruyter-Spira, C., et al. (2013) CAROTENOID CLEAVAGE DIOXYGENASE 7 modulates plant growth, reproduction, senescence, and determinate nodulation in the model legume *Lotus japonicus*. *J. Exp. Bot.* 64: 1967–1981. https://doi.org/10.1093/JXB/ERT056.

Liu, X., Hu, Q., Yan, J., Sun, K., Liang, Y., Jia, M., et al. (2020) ζ-Carotene isomerase suppresses tillering in rice through the coordinated biosynthesis of strigolactone and abscisic acid. *Mol. Plant* 13: 1784–1801. https://doi.org/10.1016/J.MOLP.2020.10.001.

Lykke-Andersen, S. and Jensen, T.H. (2015) Nonsense-mediated mRNA decay: an intricate machinery that shapes transcriptomes. *Nat. Rev. Mol. Cell Biol.* 16: 665–677. https://doi.org/10.1038/nrm4063.

Mageroy, M.H., Tieman, D.M., Floystad, A., Taylor, M.G. and Klee, H.J. (2012) *A Solanum lycopersicum* catechol-*O*-methyltransferase involved in synthesis of the flavor molecule guaiacol. *Plant J.* 69: 1043–1051. https://doi.org/10.1111/J.1365-313X.2011.04854.X.

Mashiguchi, K., Seto, Y. and Yamaguchi, S. (2021) Strigolactone biosynthesis, transport and perception. *Plant J.* 105: 335–350. https://doi.org/10.1111/tpj.15059.

Miura, H., Ochi, R., Nishiwaki, H., Yamauchi, S., Xie, X., Nakamura, H., et al. (2022) Germination stimulant activity of isothiocyanates on *Phelipanche* spp. *Plants* 11: 11. https://doi.org/10.3390/plants11050606.

Parisi, M., Pentangelo, A., D'Alessandro, A., Festa, G., Francese, G., Navarro, A., et al. (2023) Grafting effects on bioactive compounds, chemical and agronomic traits of 'Corbarino' tomato grown under greenhouse healthy conditions. *Hortic. Plant J.* 9: 273–284. https://doi.org/10.1016/J.HPJ.2022.03.001.

Qiu, D., Diretto, G., Tavazza, R. and Giuliano, G. (2007) Improved protocol for *Agrobacterium* mediated transformation of tomato and production of transgenic plants containing carotenoid biosynthetic gene *CsZCD*. *Sci. Hortic.* 112: 172–175. https://doi.org/10.1016/j.scienta.2006.12.015.

Rambla, J.L., Medina, A., Fernández-del-Carmen, A., Barrantes, W., Grandillo, S., Cammareri, M., et al. (2017) Identification, introgression, and validation of fruit volatile QTLs from a red-fruited wild tomato species. *J. Exp. Bot.* 68: 429–442. https://doi.org/10.1093/jxb/erw455.

Rasmussen, A., Mason, M.G., De Cuyper, C., Brewer, P.B., Herold, S., Agusti, J., et al. (2012) Strigolactones suppress adventitious rooting in *Arabidopsis* and pea. *Plant Physiol.* 158: 1976–1987. https://doi.org/10.1104/pp.111.187104.

Ron, M., Kajala, K., Pauluzzi, G., Wang, D., Reynoso, M.A., Zumstein, K., et al. (2014) Hairy root transformation using *Agrobacterium* rhizogenes as a tool for exploring cell type-specific gene expression and function using tomato as a model. *Plant Physiol.* 166: 455–469. https://doi.org/10.1104/pp.114.239392.

Saucet, S.B. and Shirasu, K. (2016) Molecular parasitic plant–host interactions. *PLoS Pathog.* 12: e1005978. https://doi.org/10.1371/journal.ppat.1005978.

Seto, Y., Sado, A., Asami, K., Hanada, A., Umehara, M., Akiyama, K., et al. (2014) Carlactone is an endogenous biosynthetic precursor for strigolactones. *Proc. Natl. Acad. Sci. USA* 111: 1640–1645. https://doi.org/10.1073/pnas.1314805111.

Takei, S., Uchiyama, Y., Bürger, M., Suzuki, T., Okabe, S., Chory, J., et al. (2023) A divergent clade KAI2 protein in the root parasitic plant *Orobanche minor* is a highly sensitive strigolactone receptor and is involved in the perception of sesquiterpene lactones. *Plant Cell Physiol.* 64: 996–1007. https://doi.org/10.1093/PCP/PCAD026.

Thieme, C.J., Rojas-Triana, M., Stecyk, E., Schudoma, C., Zhang, W., Yang, L., et al. (2015) Endogenous *Arabidopsis* messenger RNAs transported to distant tissues. *Nat. Plants* 1:4 1: 15025. https://doi.org/10.1038/nplants.2015.25.

Tieman, D., Zeigler, M., Schmelz, E., Taylor, M.G., Rushing, S., Jones, J.B., et al. (2010) Functional analysis of a tomato salicylic acid methyl transferase and its role in synthesis of the flavor volatile methyl salicylate. *Plant J.* 62: 113–123. https://doi.org/10.1111/J.1365-313X.2010.04128.X.

Tikunov, Y.M., Molthoff, J., de Vos, R.C.H., Beekwilder, J., van Houwelingen, A., van der Hooft, J.J.J., et al. (2013) NON-SMOKY GLYCOSYLTRANSFERASE1 prevents the release of smoky aroma from tomato fruit. *Plant Cell* 25: 3067–3078. https://doi.org/10.1105/tpc.113.114231.

Tolnai, Z., Sharma, H. and Soós, V. (2024) D27-like carotenoid isomerases: at the crossroads of strigolactone and abscisic acid biosynthesis. *J. Exp. Bot.* 75: 1148–1158. https://doi.org/10.1093/jxb/erad475.

Uauy, C., Nelissen, H., Chan, R.L., Napier, J.A., Seung, D., Liu, L., et al. (2025) Challenges of translating *Arabidopsis* insights into crops. *Plant Cell* 37: koaf059. https://doi.org/10.1093/PLCELL/KOAF059.

Umehara, M., Hanada, A., Magome, H., Takeda-Kamiya, N. and Yamaguchi, S. (2010) Contribution of strigolactones to the inhibition of tiller bud outgrowth under phosphate deficiency in rice. *Plant Cell Physiol.* 51: 1118–1126. https://doi.org/10.1093/PCP/PCQ084.

Visentin, I., Ferigolo, L.F., Russo, G., Korwin Krukowski, P., Capezzali, C., Tarkowská, D., et al. (2024) Strigolactones promote flowering by inducing the miR319-*LA-SFT* module in tomato. *Proc. Natl. Acad. Sci. USA* 121: 1–10. https://doi.org/10.1073/pnas.2316371121.

Visentin, I., Pagliarani, C., Deva, E., Caracci, A., Turečková, V., Novák, O., et al. (2020) A novel strigolactone-miR156 module controls stomatal behaviour during drought recovery. *Plant Cell Environ.* 43: 1613–1624. https://doi.org/10.1111/pce.13758.

Vogel, J.T., Walter, M.H., Giavalisco, P., Lytovchenko, A., Kohlen, W., Charnikhova, T., et al. (2010) SlCCD7 controls strigolactone biosynthesis, shoot branching and mycorrhiza-induced apocarotenoid formation in tomato. *Plant J.* 61: 300–311. https://doi.org/10.1111/j.1365-313X.2009.04056.x.

Vurro, M., Boari, A., Thiombiano, B. and Bouwmeester, H. (2019) Strigolactones and parasitic plants. In *Strigolactones - Biology and Applications*,

pp. 89–120. Springer International Publishing, https://doi.org/10.1007/978-3-030-12153-2_3.

Wakabayashi, T., Hamana, M., Mori, A., Akiyama, R., Ueno, K., Osakabe, K., et al. (2019) Direct conversion of carlactonoic acid to orobanchol by cytochrome P450 CYP722C in strigolactone biosynthesis. *Sci. Adv.* 5: 1–10. https://doi.org/10.1126/sciadv.aax9067.

Wakabayashi, T., Moriyama, D., Miyamoto, A., Okamura, H., Shiotani, N., Shimizu, N., et al. (2022) Identification of novel canonical strigolactones produced by tomato. *Front. Plant Sci.* 13: 1064378. https://doi.org/10.3389/fpls.2022.1064378.

Wang, Y., Durairaj, J., Suárez Duran, H.G., van Velzen, R., Flokova, K., Liao, C.Y., et al. (2022) The tomato cytochrome P450 CYP712G1 catalyses the double oxidation of orobanchol en route to the rhizosphere signalling strigolactone, solanacol. *New Phytol.* 235: 1884–1899. https://doi.org/10.1111/NPH.18272.

Waters, M.T., Brewer, P.B., Bussell, J.D., Smith, S.M. and Beveridge, C.A. (2012) The *Arabidopsis* ortholog of rice DWARF27 acts upstream of MAX1 in the control of plant development by strigolactones. *Plant Physiol.* 159: 1073–1085. https://doi.org/10.1104/pp.112.196253.

Wu, H., Li, H., Chen, H., Qi, Q., Ding, Q., Xue, J., et al. (2019) Identification and expression analysis of strigolactone biosynthetic and signaling genes reveal strigolactones are involved in fruit development of the woodland strawberry (*Fragaria vesca*). *BMC Plant Biol.* 19: 1–19. https://doi.org/10.1186/s12870-019-1673-6.

Yang, Y., Abuauf, H., Song, S., Wang, J.Y., Alagoz, Y., Moreno, J.C., et al. (2023) The *Arabidopsis* D27-LIKE1 is a *cis* / *cis* / *trans* -β-carotene isomerase that contributes to Strigolactone biosynthesis and negatively impacts ABA level. *Plant J.* 113: 986–1003. https://doi.org/10.1111/tpj.16095.

Ye, F., Fang, H., Feng, L., Shi, M., Yang, R. and Liao, W. (2024) Hydrogen-rich water enhanced salt tolerance in tomato seedlings by regulating strigolactone biosynthesis genes *SlMAX1* and *SlD27*. *Plant Soil* 507: 729–747. https://doi.org/10.1007/s11104-024-06767-8.

Yıldırım, K., Kavas, M., Akın, M., Küçük, İ.S. (2024). Genome editing-based strategies used to enhance crop resistance to parasitic weeds. *In A Roadmap for Plant Genome Editing*. pp. 411–422. Springer Nature Switzerland, Cham. https://doi.org/10.1007/978-3-031-46150-7_24

Yoder, J.I. and Scholes, J.D. (2010) Host plant resistance to parasitic weeds; recent progress and bottlenecks. *Curr. Opin. Plant Biol.* 13: 478–484. https://doi.org/10.1016/j.pbi.2010.04.011.

Yoneyama, K., Xie, X., Nomura, T., Yoneyama, K. and Bennett, T. (2022) Supra-organismal regulation of strigolactone exudation and plant development in response to rhizospheric cues in rice. *Curr. Biol.* 32: 3601–3608.e3. https://doi.org/10.1016/J.CUB.2022.06.047.

Yoneyama, K., Yoneyama, K., Takeuchi, Y. and Sekimoto, H. (2007) Phosphorus deficiency in red clover promotes exudation of orobanchol, the signal for mycorrhizal symbionts and germination stimulant for root parasites. *Planta* 225: 1031–1038. https://doi.org/10.1007/s00425-006-0410-1.

Zhang, Y., Cheng, X., Wang, Y., Díez-Simón, C., Flokova, K., Bimbo, A., et al. (2018) The tomato MAX1 homolog, SlMAX1, is involved in the biosynthesis of tomato strigolactones from carlactone. *New Phytol.* 219: 297–309. https://doi.org/10.1111/nph.15131.

Zhou, F., Last, R.L. and Pichersky, E. (2021) Degradation of salicylic acid to catechol in *Solanaceae* by SA 1-hydroxylase. *Plant Physiol.* 185: 876–891. https://doi.org/10.1093/PLPHYS/KIAA096.

Plant and Cell Physiology, 2026, 00(00),1–18. https://doi.org/10.1093/pcp/pcag042
Special Issue - Regular Paper